Simulation of the Knee Joint Motion by Stewart Platform

Ammar Tareq Najeeb Al-Khaffaf

Submitted to the
Institute of Graduate Studies and Research
in partial fulfillment of the requirements for the Degree of

Master of Science
in
Mechanical Engineering

Eastern Mediterranean University
October 2014
Gazimağusa, North Cyprus

Approval of the Institute of Graduate Studies and Research

Prof. Dr. Elvan Yılmaz
Director

I certify that this thesis satisfies the requirements as a thesis for the degree of Master of Science in Mechanical Engineering.

Prof. Dr. Uğur Atikol
Chair, Department of Mechanical Engineering

We certify that we have read this thesis and that in our opinion it is fully adequate in scope and quality as a thesis for the degree of Master of Science in Mechanical Engineering.

Assist. Prof. Dr. Neriman Özada
Supervisor

Examining Committee

1. Assoc. Prof. Dr. Hasan Hacışevki

2. Assist. Prof. Dr. Mostafa Ranjbar

3. Assist. Prof. Dr. Neriman Özada

ABSTRACT

The knee is one of the most commonly studied human body joints in the field of biomechanics. Biomechanical knee joint studies aim to understand joint mechanics by utilizing kinematics and dynamics. Understanding the mechanics of intact joints provides insight into the mechanics of injured, deteriorated and reconstructed joints and help to improve current technologies in the field of orthopedics. The aim of this project is to model a Steward Platform (SP) with six degrees of freedom (6DOF) based on the kinematics of anatomic knee joint. The constructed inverse kinematics equations for the SP can then predict the anatomic knee joint kinematics and major knee joint ligaments length changing. The model of the SP was used to perform the knee joint kinematics motion within a certain range of movement between 0° to 30° flexion. This application leads to investigate the similarity between the changes in the platform actuator leg lengths and the knee joint ligament lengths. The initial lengths of the platform actuator legs were adjusted to 170 mm at 0° joint flexion. Then the platform angle changes were applied to extend it up to 30° flexion angle through taking into account the center of mass (COM) of the SP. The COM of the platform was assumed as the COM of the tibia bone of the knee joint and based on the kinematic movement of the platform the lengths of actuator legs were analyzed.

From the constructed inverse kinematics equations, the SP mimicked the anatomic knee joint kinematics and the platform actuator legs predicted the anatomic knee joint ligament length changes. It was found that the lengths of the platform actuator legs varied with knee joint flexion angles during the platform motion. Also it was seen that between 0° to 30° flexion, the platform performed valgus rotation dominantly and the

actuator leg lengths decreased which represented the Anterior Cruciate Ligament (ACL), Medial Collateral Ligament (MCL), and Lateral Collateral Ligament (LCL). The average changes of the platform actuator legs were found as 0.119% for actuator leg 1, 0.035% for actuator leg 2, 0.1285% for actuator leg3, 0.1285% for actuator leg4, 0.035% for actuator leg5 and 0.119% for actuator leg6.

The current findings were compared with the literature data and the kinematics of the SP and the changes in the platform actuator legs were validated. The total time of the analysis and the simulation took two hours. Using modelling based study such as the SP model can provide an insight into the biomechanics and the orthopaedics field to reveal the knee joint kinematics and ligament length changes without using cadavers or invasive experiments.

Keywords: Stewart platform, Kinematics, Knee, Biomechanics.

ÖZ

Diz eklemi, biyomekanik alanında en fazla çalışılan insan eklemlerinden biridir. Biyomekanik alanındaki diz eklemi çalışmaları kinematik ve dinamik kullanılarak eklemin mekaniğini anlamak için yapılmaktadır. Sağlam eklem mekaniğini anlamak, yaralı, bozulan ve yenilenen diz eklemlerinin de mekaniklerini anlamaya ve ortopedi alanındaki teknolojileri geliştirmeye yardım eder. Bu projenin amacı, altı serbestlik derecesi olan diz eklemi kinematiğini sağlayabilen Steward Platform`u (SP) modellemektir. SP için kurulan ters kinematik denklemler hem anatomik diz eklemi kinematiğini hem de diz liflerinin veya bağlarının uzama ve kısalmalarını öngörebilecektir. Kurulan SP modeli ve kinematik denklemler, platformun 0° ile 30° arasındaki bükülme hareketini sağlaması için kurulmuştur. Bu aralıktaki bükülme hareketi, platformun hem anatomik diz kinematiğini hem de diz bağlarının uzama ve kısalmalarını çalışmak için yararlı olmuştur. Diz bağlarının uzunluk değişikliklerini ölçmek için kullanılacak olan platform bacaklarının başlangıç uzunlukları 0° de 170 mm olarak ayarlandı. Daha sonra platformun kütle merkezi baz alınarak, platformun açısı 30° olacak şekilde hareket ettirildi ve bacaklardan elde edilen uzunluk değişiklikleri kaydedildi. Platformun kütle merkezi, anatomik kaval kemiğinin kütle merkezi olarak uygulandı ve analizler de bu kütle merkezine göre yapıldı. Yapılmış olan analizlere göre, kurulan ters kinematik denklemler, platformun anatomik diz eklemi kinematiğini ve diz bağlarının uzunluk değişikliklerini taklit edebilecek bir model olduğunu doğruladı. Elde edilen sonuçlara göre, hem taklit edilen anatomik diz kinematiğinin hem de diz bağlarının uzunluklarının 0° ile 30° arasında değişiklikler gösterdiği de gözlendi. Bunun yanında, 0° ile 30° bükülme hareketinde, platformun valgus hareketini de yoğun olarak gerçekleştirdiği ve platform bacaklarının kısalma

gösterdiği belirlendi. Bu kısalmaların da dizdeki ön çapraz bağ, iç yan bağ ve dış yan bağı temsil ettiği anlaşıldı. Platform bacaklarının ortalama uzunluk değişiklikleri bacak 1 için 0.119%, bacak 2 için 0.035%, bacak 3 için 0.1285%, bacak 4 için 0.1285%, bacak 5 için 0.035% ve bacak 6 için 0.119% olarak elde edildi. Elde edilen sonuçlar daha önce yayınlanan çalışmalardaki veriler ile karşılaştırıldı ve platform kinematiği ile platform bacaklarının uzama ve kısalmaları geçerlilik kazandı. Toplam analiz ve simülasyon süresi iki saat sürdü.

Sonuç olarak SP gibi modelleme bazlı çalışmalar biyomekanik ve ortopedi alanlarına, kadaver ve fiziksel deneylere gerek duyulmadan, diz ekleminin kinematiği ve bağların hareketlerine ışık tutabilir ve pekçok çalışmaya da öncü olabilir.

Anahtar Kelimeler: Stewart platform, Kinematik, diz, biyomekanik.

DEDICATION

To My Family

To my dear parents, you were and will always be the light in the darkness of life

My Dear Father, My Dear Mother

and to

My Dear Brothers

ACKNOWLEDGMENT

I would like to thank Assist. Prof. Dr. Neriman Özada for her continuous support and guidance in the preparation of this study. Without her invaluable supervision, all my efforts could have been short-sighted.

I also like to thank the Department of Mechanical Engineering for valuable support.

Also I like to thank all my friends who support me and specially my dear friend Mr. Hashem Alhendi.

And finally I like to thank my dear family for their continuous support to me.

TABLE OF CONTENTS

LIST OF TABLES

LIST OF FIGURES

LIST OF ABBREVIATIONS

SP	Stewart platform
CT	Computed Tomography
6DOF	Six Degrees of Freedom
MRI	Magnetic Resonance Image
2D	Two Dimensional
3D	Three Dimensional
CAD	Computer Aided Design
1DOF	One Degree of Freedom
COM	Center of Mass
LIDS	Low Impact Docking System
NASA	National Aeronautics and Space Administration
SIMM	Software for Interactive Musculoskeletal Modeling
MV	Manipulated Variable
SIMM	Software for Interactive Musculoskeletal Modeling
PID	Proportional-Integral-Derivative
ACL	Anterior Cruciate Ligament
PCL	Posterior Cruciate Ligament
LCL	Lateral Cruciate Ligament
MCL	Medial Cruciate Ligament
VV	Varus – Valgus
IE	Internal-External

LIST OF SYMBOLS

k_p	Proportional gain
k_i	Integral gain
k_d	Derivative gain
e	Error
SP	Set –point
PV	Present value
t	Present time
τ	Variable of integration (0 - t)
$u(t)$	Controller output
$\mathrm{MV}(t)$	Manipulated variable
θ_b	Base triangle angles
θ_p	Platform triangle angles
F_i (F_1-F_6)	Connecting points of legs to the base
M_i (M_1-M_6)	Connecting points of legs to the platform
R_m	Radius of the moving platform
R_f	Radius of the fixed base
P	Position vector
${}^{F}R_M$	Rotation matrix
F_{xyz}	coordinate systems of the fixed base
M_{xyz}	coordinate systems of the platform
l_i	length of the SP leg

GM_i	position vectors of upper platform
GF_i	position vectors of the base
G_{p-o}	Position and orientation of the platform

Chapter 1

INTRODUCTION

1.1 Robotic Systems in Orthopaedic Field

Since the surgery is one of the most dangerous and risky treatment for people, it requires reliable products. Therefore, due to their high accuracy, robots have been used in the field of orthopedic surgery.

However, robots didn't appear in the field of orthopedics until about mid-80s when the world's first surgical robot the (Arthobot) was used for the first time in Canada in 1983. The Arthobot was developed by a team in collaboration with orthopedic surgeons. Then new robots started to reveal like PUMA 200 which was used to put a needle in a brain to take a biopsy with the help of CT (Computed Tomography) guidance [1]. Robots like PROBOT, ROBODOC and Da Vinci Surgical System are examples of currently used robots in medical surgeries [2].

Using of robots in surgical operations increased the speed and accuracy of surgical operations.

Medical and surgical robots started to participate in different fields of surgeries and started to give remarkable results.

Orthopaedic surgery was one of these fields where the robots started to play a major roles in it. The most of orthopedic surgeries are performed to straighten a bone deformation, extending bone length, removing parts of the bones affected by infections or tumors, and replacing human joint components.

When computer-assisted robotic systems entered to these operations, a big differences in the amount of precision and accuracy were seen.

Different robotic systems for orthopaedic surgery have been revealed and developed. In general there were two types of robots; first one was the serial manipulator like Robodoc, Caspar, Acrobot and Arthrobot and the second one was the parallel manipulator like Orthdoc, NonaPod, and MBARS.

The Six-Axis Correction External Fixation Devices which uses a computer-dependent Stewart platform as a modified version of the essential Ilizarov device [3] is also widely used.

In general, each robot has its advantages and disadvantages, but the parallel robots has specific advantages over serial robots, such as better stiffness and precise positioning capability.

Parallel manipulators are closed kinematic structures having the requisite rigidity to yield a high payload to self-weight ratio unlike the serial ones which has a lower stiffness and less accuracy and possess a low nominal

load-weight ratio. Therefore, most of the current studies aim to develop parallel robots as it has better potential over the serial ones.

In this project, it is aimed to model a parallel robot which is the Stewart Platform to mimic the human knee joint motion and determine the relation between the platform actuator leg lengths and the knee joint ligament lengths.

The purpose is to compare the changes in the ligament lengths and the platform actuator legs and compare the kinematics of the Stewart Platform with the anatomic knee joint kinematics to benefit from it in medical applications such as rehabilitation, designing prostheses, orthopaedic surgeries, etc.

1.2 Human Knee Joint Modeling and Simulation

The knee joint is one of the most and greatest demanded joint in human body, and it always motivates researchers to study the knee joint and understand the mechanism of it to reach better results in dealing with knee cases like injuries, diseases, and reconstruction.

Nowadays modeling and simulation for any project in any scope of science became a basic step to analyze the data or the model of the project to give a thorough and futuristic expectation about the final results.

For example, when designing implants, simulation offers many advantages opposed to experiments. In the orthopaedics field, knowing the muscle forces acting upon a fracture is crucial for designing a fixation device to

make a decision whether the bone should be supported from the bottom or the top. This problem can be solved with the modeling analysis.

As the knee joint is one of the most problematic joint, it became one of the gravity point for most of current orthopedic researchers to focus on the joint movements in different activities like sport activates to get a better understanding.

The knee joint consists of femur and tibia which is known as the tibio-femoral joint. It also consists of fibula and patella or kneecap bone.

The knee joint has a complex architecture formed by nonsymmetrical surfaces and its movement is more complicated than just a revolute joint motion, which performs 6DOF movement.

The first step to analyze the knee joint is constructing a model for it to be analyzed using different computer software. Geometrical models of anatomical parts are difficult to be obtained and manipulate, especially because their irregular surfaces. To construct a model of a knee joint, it should pass many steps, starting with taking MRI (magnetic resonance image) or CT scan of the real bone of patient to get 2D (two dimensional) medical images.

Second step is converting these 2D images to 3D (three dimensional) images using special programs like 3D slicer or sliceOmatic. These give a cumulative 3D images and by using the same programs, extension of the

image file can be changed to one of CAD (Computer aided design) files to be used by other CAD modeling programs. To finalize the geometry of the model, a specialized CAD shaping program must be used and one of these programs is Geomagic (430 Davis Drive, Morrisville, NC, USA) [4]. After having a complete model of a bone or a joint, analyzing the movement can be configured by one of dynamic or kinematic simulation analysis program like OpenSim [5] [6].

In general, the knee joint is considered as a hinged joint with 1DOF and that means it only performs flexion/extension. However, from the kinematics point of view, it has three dimensional rotations and three dimensional translations.

It has a combined motion with flexion/extension being the main movement (rotation around x axis), abduction-adduction rotations (rotation around y axis), internal-external rotations (rotations around z axis) and the remaining degrees of freedom are the superior-inferior translations (translation along z axis), medial-lateral translation (translation along y axis) and anterior-posterior translations (translation along x axis). Therefore, any constructed knee joint model should include all these 3D translations and 3D rotations to perform realistic joint simulations.

Therefore, one of the aims of this project is to model a Steward Platform which has 6DOF movement like a knee joint. Then, the model of the Steward Platform is used to perform the knee joint kinematic motion from 0° to 30° to investigate the similarity between the changes in the platform leg lengths and the knee joint ligament lengths. Using the Steward Platform model will provide an insight into the biomechanics and

the orthopaedics field to reveal the knee joint kinematics and ligament length changes without using cadavers or invasive experiments.

1.3 Knee Joint Anatomy

The knee joint has three parts. The thigh bone (the femur) meets the large shin bone (the tibia) to form the main knee joint. This joint has an inner (medial) and an outer (lateral) compartment. The kneecap (the patella) joins the femur to form a third joint, called the patellofemoral joint. The patella protects the front of the knee joint.

The knee joint is surrounded by a joint capsule with ligaments strapping the inside and outside of the joint (collateral ligaments) as well as crossing within the joint (cruciate ligaments). The collateral ligaments run along the sides of the knee and limit the sideways motion of the knee. The anterior cruciate ligament (ACL) connects the tibia to the femur at the center of the knee and functions to limit rotation and forward motion of the tibia. The posterior cruciate ligament (PCL) located just behind the ACL limits the backward motion of the tibia, besides ACL and PCL there are the MCL and the LCL ligaments, All of these ligaments provide stability and strength to the knee joint.

The meniscus is a thickened cartilage pad between the two joints formed by the femur and tibia. The meniscus acts as a smooth surface for the joint to move on. The knee joint is surrounded by fluid- filled sacs called bursae, which serve as gliding surfaces that reduce friction of the tendons. Below the kneecap, there is a large tendon (patellar tendon) which attaches to the front of the tibia bone. There are large blood vessels passing through the area behind the knee. The large muscles of the thigh move the knee. In the front of the thigh the quadriceps muscles extend the knee joint. In the back

of the thigh, the hamstring muscles flex the knee. The knee also rotates slightly under guidance of specific muscles of the thigh.

1.3.1 Knee Ligament Anatomy

The knee joint is a vulnerable joint that is easily injured and this is due in part to the fact that the joint is well exposed and in the middle of two long lever-arms, the femur and tibia. Unlike the hip joint which has a very stable ball-and-socket configuration, the bone anatomy of the knee imparts little support to the joint's stability. This makes the knee ligaments prone to injury with any contact to the knee, or often with just the force of a hard muscle contraction (e.g. performing a quick change of direction when sprinting) making the ligaments injuries one of the very common injuries to the knee (especially for athletes) so the understanding of ligaments anatomy is important to predict the shape of the movement of the knee.

There are essentially four separate ligaments that stabilize the knee joint, on the sides of the joint lie the medial collateral ligament (MCL) and the lateral collateral ligament (LCL) which serve as stabilizers for the side-to-side stability of the joint. The MCL is a broader ligament that is actually made up of two ligament structures, the deep and superficial components, whereas the LCL is a distinct cord-like structure.

In the front part of the center of the joint is the anterior cruciate ligament (ACL), this ligament is a very important stabilizer of the femur on the tibia and serves to prevent the tibia from rotating and sliding forward during agility, jumping, and deceleration activities, directly behind the ACL is its opposite, the posterior cruciate ligament (PCL), the PCL prevents the tibia from sliding to the rear.

1.4 Organization of the Thesis

In this thesis, Chapter 1 consists of the introduction about the robots in orthopedics field and the modeling and simulation applications of the knee joint, besides the anatomy of the knee joint.

In Chapter 2, literature review is provided about the history, development and applications of robots in orthopedics field. The knee joint modeling and simulation softwares, the application of the joint modeling in medical and orthopedic fields are also explained in the Chapter 2, the construction parts of parallel robots are also demonstrated in Chapter 2.

Chapter 3 includes the steps in developing Stewart Platform model and its kinematic analysis to mimic the knee joint motion.

The results and the discussion about mimicking the knee joint kinematics with Stewart platform are written in Chapters 4.

Chapter 5 includes the conclusion about the results of this study.

Chapter 2

LITERATURE REVIEW

2.1 The History of Parallel Robots and Stewart Platform

The higher demands for general-purpose industrial robots are continuously increasing specially the robots that have the ability of application for different types of operations which require higher operational accuracy, higher load capacity and cycle time, with higher privileges that allow increasing the production.

One of the trends to achieve these requirement is using the parallel robots. Parallel robots in general consist of two platforms connected by at least two kinematic connectors that provide relative movement between a base platform (stationary) and a movable platform.

The parallel robots passed through many stages until they reach the current concepts starting from 1928, when E. Gwinnet [7] invented the first spatial parallel mechanism which was a conceptual entertainment device, however the industry didn't pay any attention at that time, and the invention was much ahead of his time and the industry was not ready for it.

After ten years, L.V. Pollard [7] have come with a design of a novel parallel robot that was used for automatic spray painting, which was the first step towards this kind of mechanisms. In fact in the parallel kinematics community, this design is known as the

first industrial parallel robot design but again the design did not get many attention by the industry. But Pollard's son, modified the design and optimized it to complete the first industrial parallel robot.

Three leading researchers (Eric Gough, D. Stewart, and Klaus Cappel) were the pioneers of parallel robots and each one of them participated in developing parallel robots.

Eric Gough who invented the six degrees of freedom (6DOF) parallel robot in 1947, revolutionized the robotic industry. The parallel robot was used as a tire-testing device to find out the characteristics of tires which are subjected to various loads. This design interpreted into a real machining in 1954. The universal tire-testing machine (universal rig) was invented in to tackle with the problems of aero-landing loads. A machine was required to detect the properties of tires under various loads. During that time, the octahedral hexapod was already existing, as mentioned by Gough [8] and Bonev [9]. Hexapods of three vertical and three horizontal jacks have been very common at that time that their origins were long forgotten.

This type of systems (and similar ones) are known as the acronym MAST [10], which represent Multi-Axis Simulation (Shake) Table, and it was well recognized in the vibration community and are still being manufactured to be used in earthquake simulations.

Gough rearranged the six struts to get a symmetrical arrangement to form an octahedron so that greater range of movement would be achieved. The modified

machine was built in the early 1950s and was fully operational in 1954. Gough's universal rig continued to be in operation until the break of the new millennium.

In 1965, a paper was published by Stewart [11] described the 6DOF motion platform which was designed to be as an aircraft simulator, which was also called "Stewart-Platform".

Stewart, [11] made many different developments from other types of hexapod mechanisms during the last decades. In fact, Stewart was the one who introduced the parallel robot into the academic environment and he contributed in popularizing the Gough's design. Furthermore Stewart's published paper [11] had a great impact on the subsequent development in the field of parallel kinematics, where various suggestions for the use of the hexapod were made.

In 1962 [7], K. Cappel, from Franklin Institute Research Laboratories in Philadelphia, worked on the same hexapod mechanism to be used as a motion simulator. After a request raised by Sikorsky Aircraft Division of United Technologies for the design and construction of a 6DOF helicopter flight simulator, the first ever flight simulator based on the octahedral hexapod was developed. Many researchers had significant roles in developing and modifying this platform and each one had his own contribution to achieve appropriate design.

Nowadays, parallel robots are used in different industrial scopes and practical applications like adjustable articulated trusses, vehicle and aircraft simulators, medical devices, and in more recently they have been used in high precision machine tools.

Also the Stewart Platform is currently used in different projects and applications around the world like LIDS (Low Impact Docking System) which was developed by NASA (National Aeronautics and Space Administration), full flight simulator cockpit, RoboCrane, satellite dish positioning for telescopes and in orthopedic surgeries.

2.2 Software Used in Modeling and Simulation of Human Body Joints

Physical-based simulation provides a powerful framework for understanding surgical and biomechanical formulations and function for different parts of human body. Modeling and simulation also helped in different branches of medical treatment especially in the orthopedics field. Nowadays different software are developed to help researchers and surgeons to achieve better results in different orthopedics cases such as planning a surgery for treating the hamstring muscle of children with cerebral palsy; knee joint arthroplasty; revealing the mechanism of movement abnormalities and gate analysis, etc.

One of the modeling and simulation software is OpenSim [5] [6], a freely available software that provides advanced modeling and simulation of human movement, including inverse and forward dynamics analyses.

OpenSim has been used in different projects around the world for different platforms, biomechanics, ergonomics and robotics for analyzing and simulating the human and animal movements to achieve solutions for different musculoskeletal problems.

Another program is SIMM (Software for Interactive Musculoskeletal Modeling, MusculoGraphics, Inc., 3617 Westwind Boulevard, Santa Rosa, California USA 95403) [12], that allows users to build models that accurately represent force generation of muscles, geometry of bones, kinematics of joints, and dynamics of joint movements.

In SIMM software, a model consists of a set of rigid segments that are connected by joints. Muscles and ligaments span the joints, develop force, and generate moments about the joints.

As these software programs are using a preloaded models in general, there are other programs and tools which are used for constructing individual models of musculoskeletal systems from magnetic resonance images (MRI) or CT scan images to be used.

One of these programs is 3D Slicer, a free, open source program, which has grown tremendously since it was developed first in late 1990's. It is used for constructing 3D geometric models of human anatomy from medical images and it has a unique ability that allows researchers to develop and add their own algorithms.

Another program for creating 3D surfaces from 2D medical images (fluoroscopic-images) is sliceOmatic (TomoVision, 3280 chemin Milletta, Magog, J1X 0R4, Canada) [13], a software for image processing from TomoVision, which produces a CAD files to be used in simulation software.

Another type of software is the one that allows to modify the CAD files like Geomagic [4], which allows for the final user to modify and improve the 3D shape to get better surface. These days Geomagic has started to enter strongly in orthopeadics field in different new projects like for making a virtual prototype to improve knee replacement design, extending life span and functionality of artificial knees and improving prosthetic shapes.

In addition to above specifications, Geomagic allows for 3D printing of the final model of the CAD file and allowing for further experimenting on the final model.

2.3 Mechanical parts of Stewart Platform

Stewart platform is a model of parallel mechanism, parallel mechanism is a closed-loop mechanism in which the end-effector is connected to the base by at least two independent kinematic chains [10]. This can be further divided into fully-parallel and hybrid mechanism. Fully-parallel mechanism is the one with an n-DOF end-effector connected to the base by n independent kinematic chains, each having a single actuated joint like SP which has a 6-DOF. The hybrid one has the combination of serial and parallel mechanisms. The fundamental common parts of parallel mechanism robots are as follow:

2.3.1 Actuators

Actuators are necessary in each robot to give the motive power for robots. Most robot actuators are available commercially, which are adapted or modified, as necessary, for a specific robot application. The three commonly used actuators are hydraulic, pneumatic, and electromagnetic.

Hydraulic actuators

Hydraulic actuators, were used as power sources for the earliest industrial robots, offer high force capability and high power-to-weight ratios. In hydraulic systems the power is provided mechanically from an electric motor or engine driven high-pressure fluid pump. This type of actuators commonly exist as linear cylinders [10], rotary vane actuators, and hydraulic motors.

The control of this type of actuators applied through a solenoid valve (on/off control) or a servo-valve (proportional control), which is driven electrically from a low-power electronic control circuit. The hydraulic power supply is bulky and the proportionally fast-response servo-valves are high in prices. Leaks and maintenance problem have limited the use and application of hydraulically powered robots.

Pneumatic Actuators

Pneumatic actuators are primarily found in simple manipulators, typically they provide uncontrolled motion between mechanical limit stops. These actuators provide good performance in point-to-point motion [10]. They are simple to control and are low in cost. Extensive use of pneumatic-actuated robots requires installation of a costly dedicated compressed-air source. Pneumatic actuators have low energy efficiency.

Proportional, closed-loop, servo-controlled pneumatic manipulators have been developed and successfully applied, principally in applications where safety, environmental and application conditions discourage electric drives. An example is an early version of the DeLaval International AB Tumba, Sweden VMS (Voluntary Milking System) cow-milking robot, which used pneumatic actuators and electro-pneumatic proportional valve joint controls in a farm, milking stall, environment

Electromagnetic Actuators

The most common types of actuators in robots today are electromagnetic actuators and there are different types of it and the most common types of it are the following ones:

Stepper Motors

Small, simple robots, such as bench-top adhesive dispensing robots, frequently use stepper or pulse motors of the permanent magnet (PM) hybrid type or sometimes the variable reluctance (VR) type. Micro-step control can produce 10 000 or more discrete robot joint positions.

In open-loop step mode the motors and robot motions have a significant settling time, which can be damped either mechanically or through the application of control algorithms, Power-to-weight ratios are lower for stepper motors than for other types of electric motors. Stepper motors operated with closed-loop control function similarly to direct-current (DC) or alternating-current (AC) servomotors.

Permanent-Magnet DC Motor

The permanent-magnet, direct-current, brush-commutated motor is widely available and comes in many different types and configurations.

The lowest-cost permanent-magnet motors use ceramic (ferrite) magnets as robot toys and hobby robots which often use this type of motor [10]. Neodymium (NEO) magnet motors have the highest energy-product magnets and in general produce the most torque and power for their size.

Ironless rotor motors, often used in small robots, typically have copper wire conductors molded into epoxy or composite cup or disk rotor structures. The advantages of these motors include low inductance, low friction and no cogging torque. Disk armature motors have several advantages. They have short overall lengths, and because their rotors have many commutation segments they produce a smooth output with low torque ripple.

A disadvantage of ironless armature motors is that they have a low thermal capacity due to low mass and limited thermal paths to their case. As a result, when driven at high power levels they have rigid duty-cycle limitations or require forced-air cooling

Brushless Motors

Also called AC servomotors or brushless DC motors, are widely used in industrial robots, they substitute magnetic or optical sensors and electronic switching circuitry for the graphite brushes and copper bar commutator, thus eliminating the friction, sparking, and wear of commutating parts. Brushless motors generally have good performance at low cost because of the decreased complexity of the motor. However, the controllers for these motors are more complex and expensive than brush-type motor controllers. The brush-less motor's passive multi-pole neodymium magnet rotor and wire-wound iron stator provide good heat dissipation and excellent reliability. Linear brushless motors function like unrolled rotary motors. They typically have a long, heavy, multiple magnet passive stator and a short, lightweight, electronically commutated wire wound forcer (slider).

Other Actuators

A wide variety of other types of actuators have been applied to robots, a sampling of these include, thermal, shape-memory alloy (SMA), bimetallic, chemical, piezoelectric, magnetostrictive, electroactive polymer (EPAM), bladder, and micro-electromechanical system (MEMS) actuators [10].

Most of these actuators have been applied to research and special application robots rather than volume production industrial robots. An example of a piezoelectric actuatr powered robot is the six-axis PI piezo hexapod with sub-nanometer resolution.

2.3.2 PID Controller

PID controllers are a family of controllers, PID controllers are used in common and are often the solution to be chosen when a controller is needed to close the loop. The reason PID controllers are so popular is that using PID gives the designer a larger number of options and those options mean that there are more possibilities for changing the dynamics of the system in a way that helps the designer to get the advantages of several effects.

Traditionally, control design in robot manipulators can be understood as the simple fact of tuning of a PD or PID compensator at the level of each motor driving the manipulator joints [14]. Fundamentally, a PD controller is a position and velocity feedback that has good closed-loop properties when applied to a double integrator system.

The PID control has a long history since Ziegler and Nichols' PID tuning rules were published in 1942 [15].

Actually, the strong point of PID control lies in its simplicity and clear physical meaning. Simple control is preferable against complex control, at least in industry.
In PID, starting with a proportional controller, and adding integral and derivative terms to the control will give the designer the advantage of the following effects:

- An integral controller gives zero SSE for a step input.
- A derivative control terms often produces faster response.

A PID controller operates on the error in a feedback system and does the following:

- A PID controller calculates a term proportional to the error - the P term.

- A PID controller calculates a term proportional to the integral of the error the I term.
- A PID controller calculates a term proportional to the derivative of the error the D term.

The three terms; P, I and D terms, are added together to produce a control signal that is applied to the system being controlled.

And the physical meanings of PID control [16] are as follows:

P-control means the present effort making a present state into desired state.

I-control means the accumulated effort using the experience information of previous states.

D-control means the predictive effort reflecting the information about trends in future states.

A PID controller calculates an error value as the difference between a measured process variable and a desired set-point. The controller attempts to minimize the error by adjusting the process through use of a manipulated variable.

The ideal version of the PID controller can be represented by the following formula

$$u(t) = \mathrm{MV}(t) = k_p\, e(t) + k_i \int_0^t e(\tau) d\tau + k_d \frac{de(t)}{dt} \qquad (2.1)$$

Where

$u(t)$: Controller output, k_p : Proportional gain, k_i : Integral gain,

k_d : Derivative gain

$$e = \mathrm{Sp} - \mathrm{PV} \qquad (2.2)$$

Where

e : error, Sp: Settling point, PV: Present Value

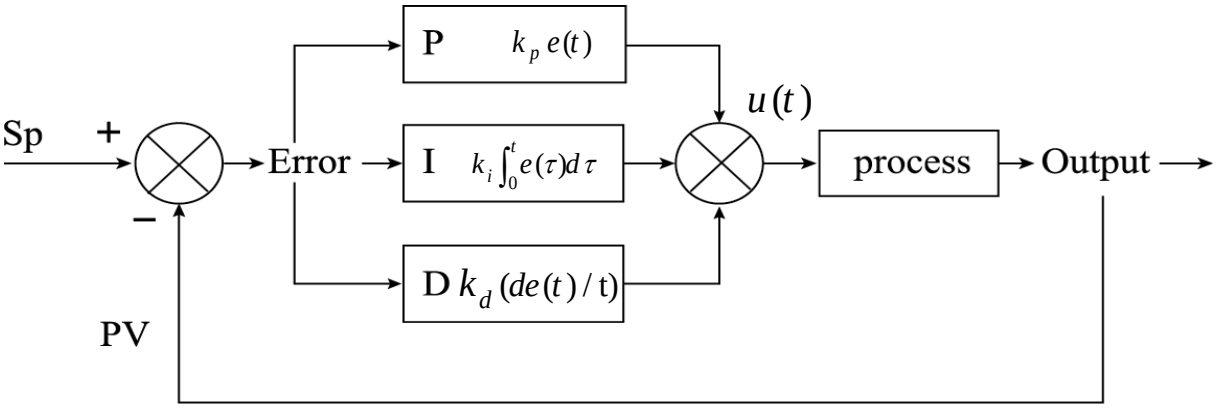

Figure 2.1: General representation of PID controller circuit

2.3.3 Joints

The most commonly used joints for parallel robots, are, in increasing order of degrees of freedom: revolute, prismatic, universal and ball-and-socket joints.

Revolute Joint (also called pin joint or hinge joint):

Revolute joint, is a one degree-of-freedom kinematic joint, provides single-axis rotation function, the revolute joint allows two components to produce relative rotation along the joint axis, the vertical dimension between the two components, is a constant value called offset distance. The vertical dimnsion and offset distace describe the spatal relative relatioship of the two componets which forms a revolute joint.

Revolute joints is the most commonly found joint in industrial robot and research robots, and it can be found in many classic applications, such as door hinges, folding mechanisms, and other uniaxial rotation devices.

Prismatic Joint (also called sliders):

A prismatic joint is a one degree-of-freedom kinematic joint, which provides single axis sliding function, a prismatic joint allows two components to produce relative displacement along the common axis. The included angle between the two components is a constant value, called deflection angle. The displacement and deflection angle describe the spatial relative relationship of the two components, which forms a prismatic joint.

Prismatic joint can be used in places such as hydraulic and pneumatic cylinders.

Universal joint (also called Hooke joint):

Universal joint allows two components to produce two degree-of-freedom relative independent rotation along two perpendicular axes. Generally, a universal joint is equivalent to two revolute joints whose axes must be completely perpendicular.

Spherical Joint (also called ball-and-socket joint):

A spherical joint allows one element to rotate freely in three dimensions with respect to the other about the center of a sphere. The sense of each rotational degree-of freedom is defined by the right-hand rule, and the three rotations together form a right-hand system. The relative pose of two components can be confirmed by three Euler angles, φ (rotate along the original z-axis), θ (rotate along the new x-axis) and ψ (rotate along the new z-axis). A spherical joint is kinematically equivalent to three intersecting revolute joints.

Chapter 3

THEORY AND MODELLING

3.1 Developing the Stewart Platform Model

The advantages of modeling and simulation include reducing the cost of studies, prototypes and getting highly accurate results. So that a Steward Platform (SP) model has been used in this project to represent and analyze the SP kinematics and investigate the knee joint kinematics.

A specialized modeling program called Wolfram SystemModeler has been used in conjunction with Mathematica (Lower Road, Long Hanborough, Oxfordshire OX29 8FD,UK) [17]. These softwares with their capabilities of modeling and simulation of data and motions in different platforms like moving bodies of machines, aerodynamics, automotive and transportation, and robotics are very popular.

Wolfram consists of two parts, the coding part which includes the ability to write and execute codes and functions and the modeling part which allows for interactive and accurate simulations of moving objects leading to the development of realistic and detailed models for a desired project.

The modeler has a big library of blocks for different scientific platform that help in modeling the shapes or data of the objects, which ensures creating quick and accurate simulations.

3.1.1 Preparation of the Stewart Platform Model

To model the SP, components of a library called Modelica.Mechanics have been used to represent the different mechanical parts of the SP.

The SP consists of a base and a moving platform with six legs. By controlling the length of these legs (actuators) the desired movement of the knee joint can be obtained. To model the SP, these parts must be constructed one by one and then gathered to complete the final shape of the model. In the following subjects, the parts of the Steward Platform are explained in more detail.

Base:

The base is the fixed part of the SP model, where the legs are connected to it. In Figure 3.1, the base part of the SP model is shown. The specifications of the base model is given in Table 3.1 as follows;

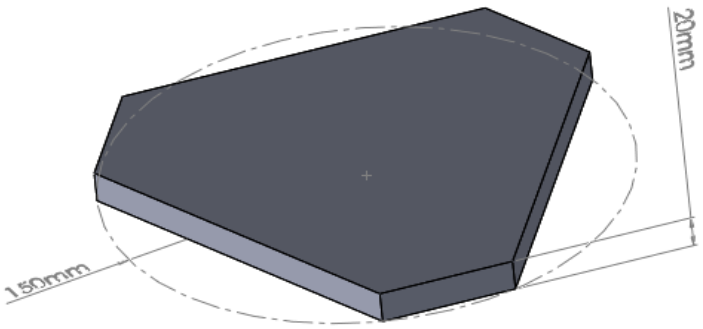

Figure 3.1: Stewart Platform Base

Table 3.1: Specifications of the Base Part

Thickness	20mm
Base radius	150mm
Base triangle angles (θ_b)	0°, 120°, 240°
Base truncation angle	15 ° θ_b ±15

As the base is connected to the legs of the platform, the Figure 3.2 shows the schematic representation of the base with the leg connections.

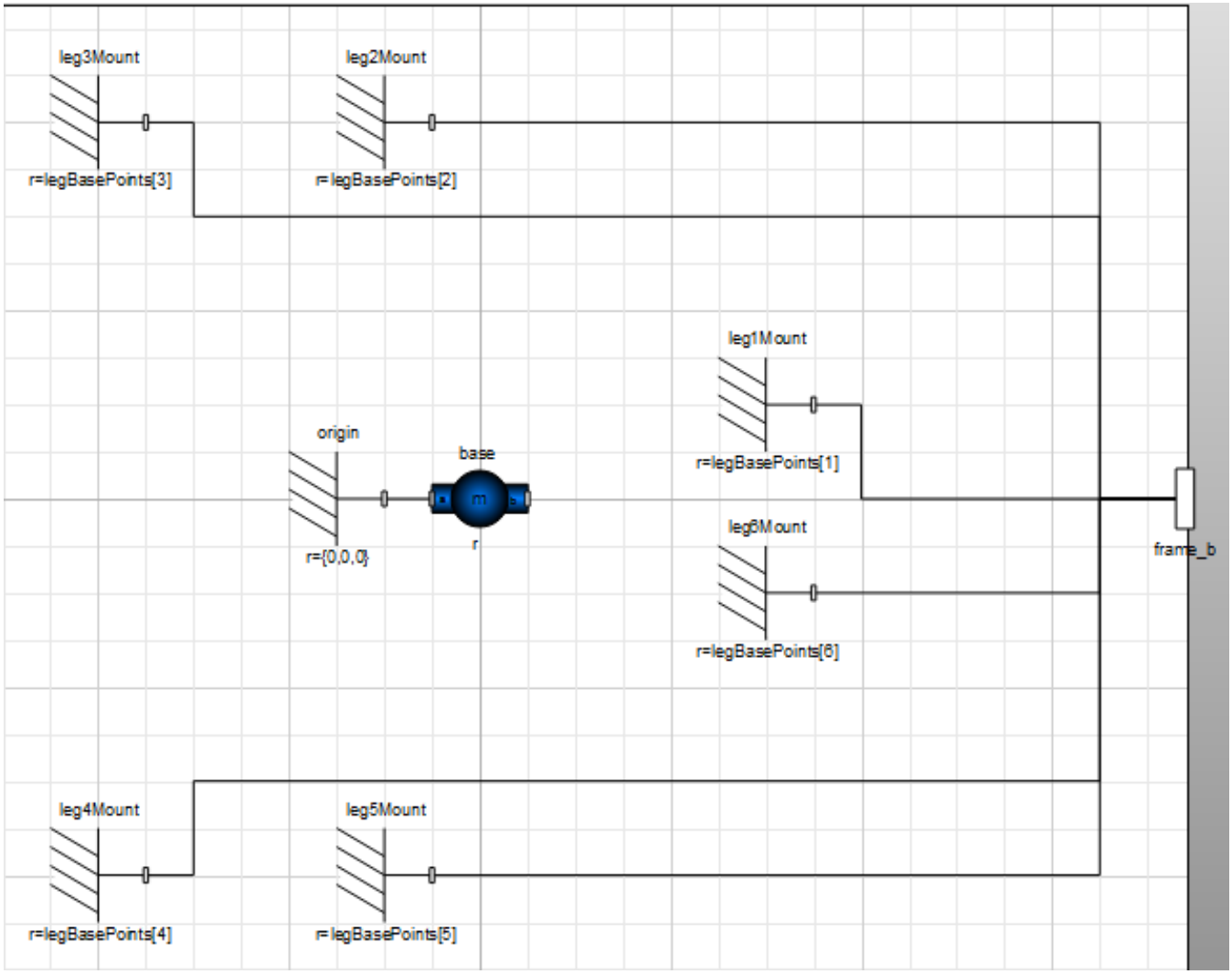

Figure 3.2: Representation of the Base of SP in Modeler System and the points of contact with the legs

Platform:

The other main part of the SP is the platform part. In Figure 3.3, the platform part of the SP model is shown. The specifications of the platform model is given in Table 3.2 as follows;

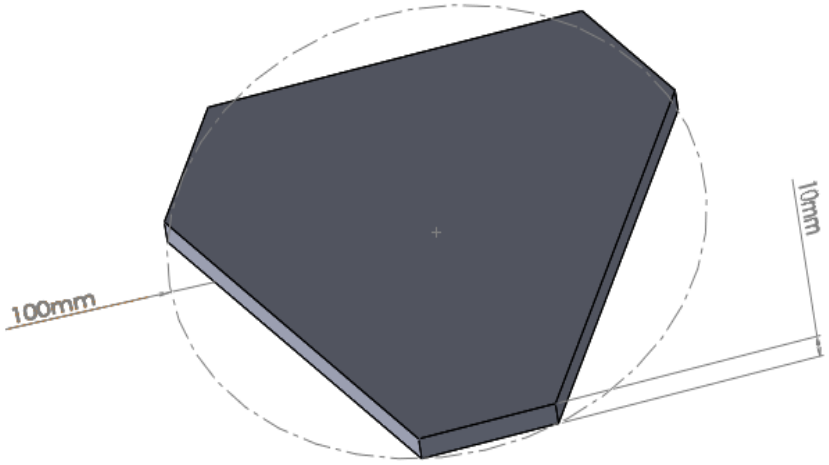

Figure 3.3: The Upper Platform of the Stewart Platform

Table 3.2: Specifications of the Upper Platform Part

Thickness	10mm
radius	100mm
Platform triangle angles (θ_p)	60°, 180°, 300°, Triangle angles shifted from base by 60°
Platform truncation angle	15 ° θ_p ±15
platform mass	1.8 kg

Figure 3.4 shows the schematic representation of the upper platform with the leg connections.

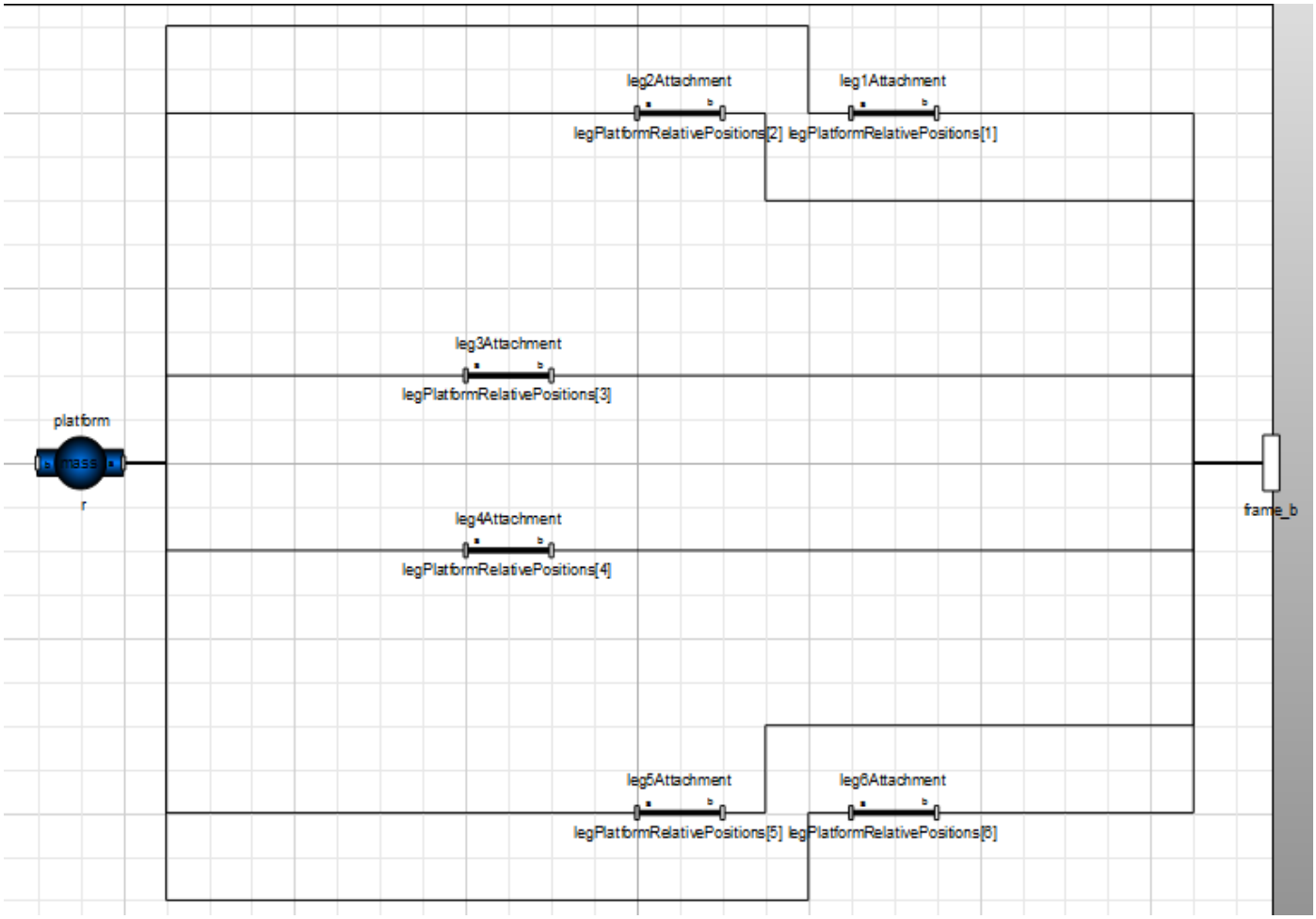

Figure 3.4 : Representation of the platform of SP in SystemModeler and the Points of Contact with the legs

Actuators (legs):

The SP model consists of actuators which represent the legs of the platform. The Actuators include three mechanical pars as listed below;

1. Two dimensional (2D) universal joint
2. One dimensional (1D) prismatic joint and its controller
3. Three dimensional (3D) spherical joint

The general schematic representation of the actuators is given in Figure 3.5 as follows;

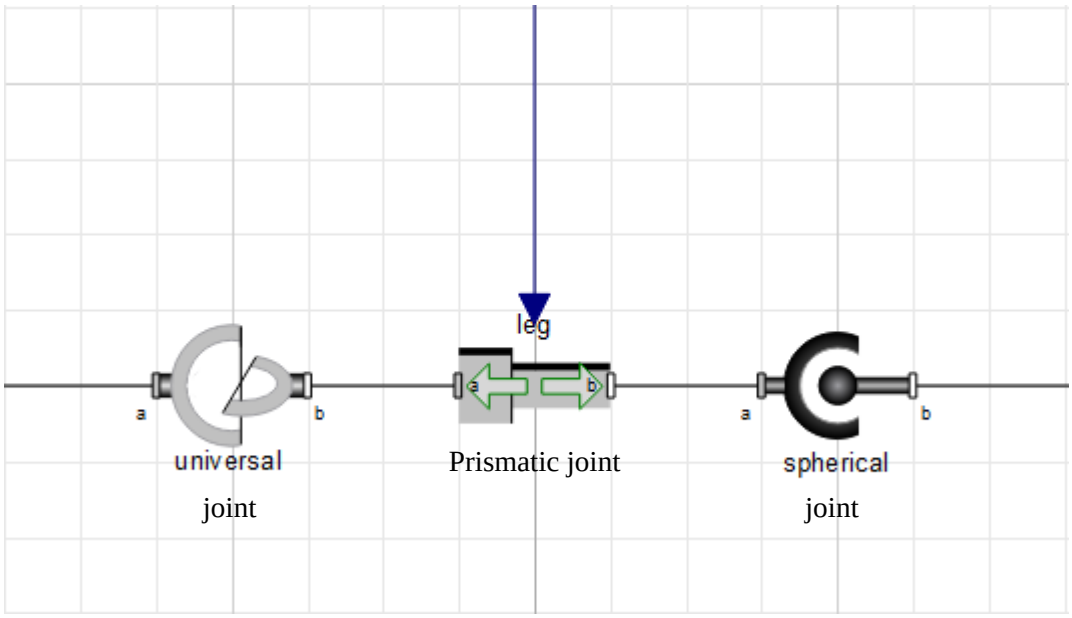

Figure 3.5: Schematic Representation of the Actuator

The connections of the controller to the actuators are also given by Figure 3.6.

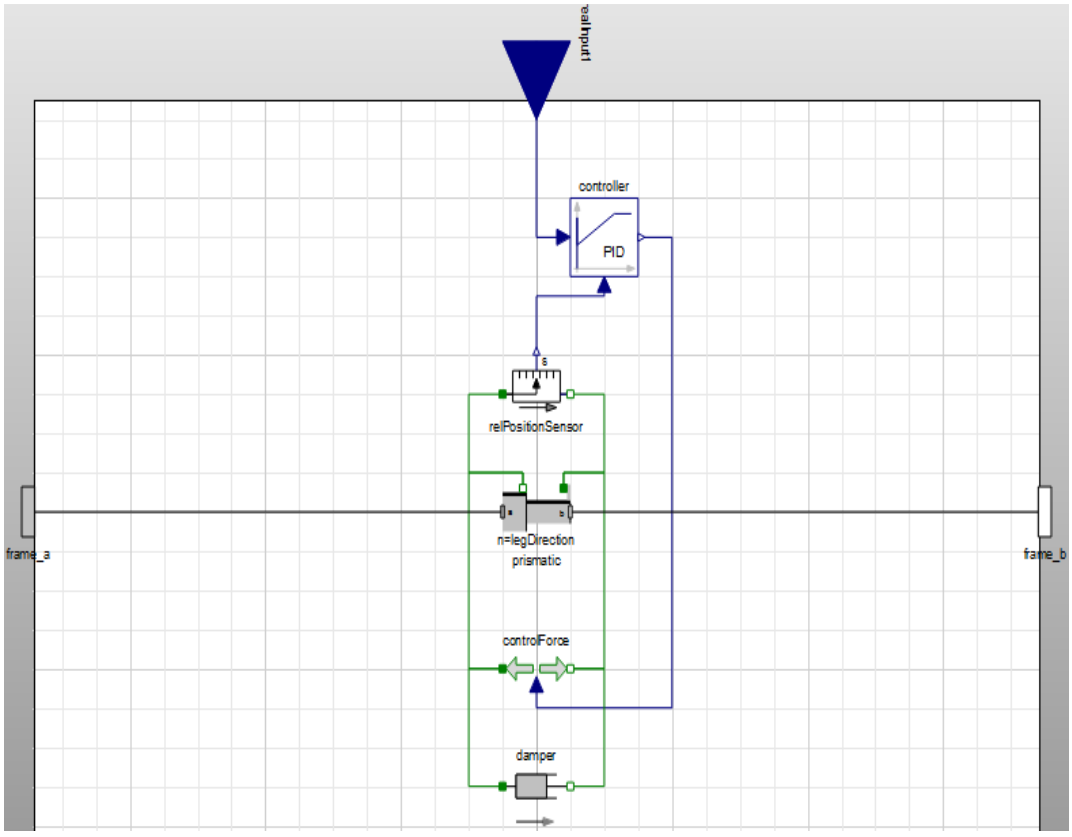

Figure 3.6: The Controller of the Prismatic Joint

3.1.2 Constructing Inverse Kinematic Equations of Stewart Platform

Parallel structure is a closed kinematic model in which all the legs are connected from the origin of the tool points by a parallel connection and this connection allows higher precision and higher velocity.

The kinematic and dynamic modeling of SP is extremely complicated in comparison with serial robots. Robot kinematics typically, can be divided into two types, forward kinematics and inverse kinematics.

For parallel manipulators, inverse kinematics is straight forward and there is no complexity deriving the equations. However, forward kinematics of SP is very complicated and difficult to solve since it requires the solution of many non-linear equations. Moreover, the forward kinematic problem generally has more than one solution.

The SP manipulator used in this study, is a 6DOF parallel mechanism model that consists of a rigid moving plate, connected to a fixed base plate through six kinematics legs. Length of the legs is variable and they can be controlled separately to perform the motion of the moving platform.

To describe the movement of the moving plate of SP, the position of attachment points of the legs with the upper platform must be represented (Fig 3.7a), and the coordinate systems for the upper and lower platforms must be constructed.

Two coordinate systems, first one (F_{xyz}) attached to the fixed base and the second one (M_{xyz}) are attached to the moving platform at each center of mass respectively. Points

(F_i and M_i) are the connecting points of legs to the base and to the platform respectively. These points are distributed on fixed and moving platforms (Fig 3.7a).

The separation angles between the points (M_1 and M_2, M_3 and M_4, M_5 and M_6) are represented by θ_m as shown in Figure (3.7b). In a similar way, the angles between the points (F_1 and F_2, F_3 and F_4, F_5 and F_6) are represented by θ_f.

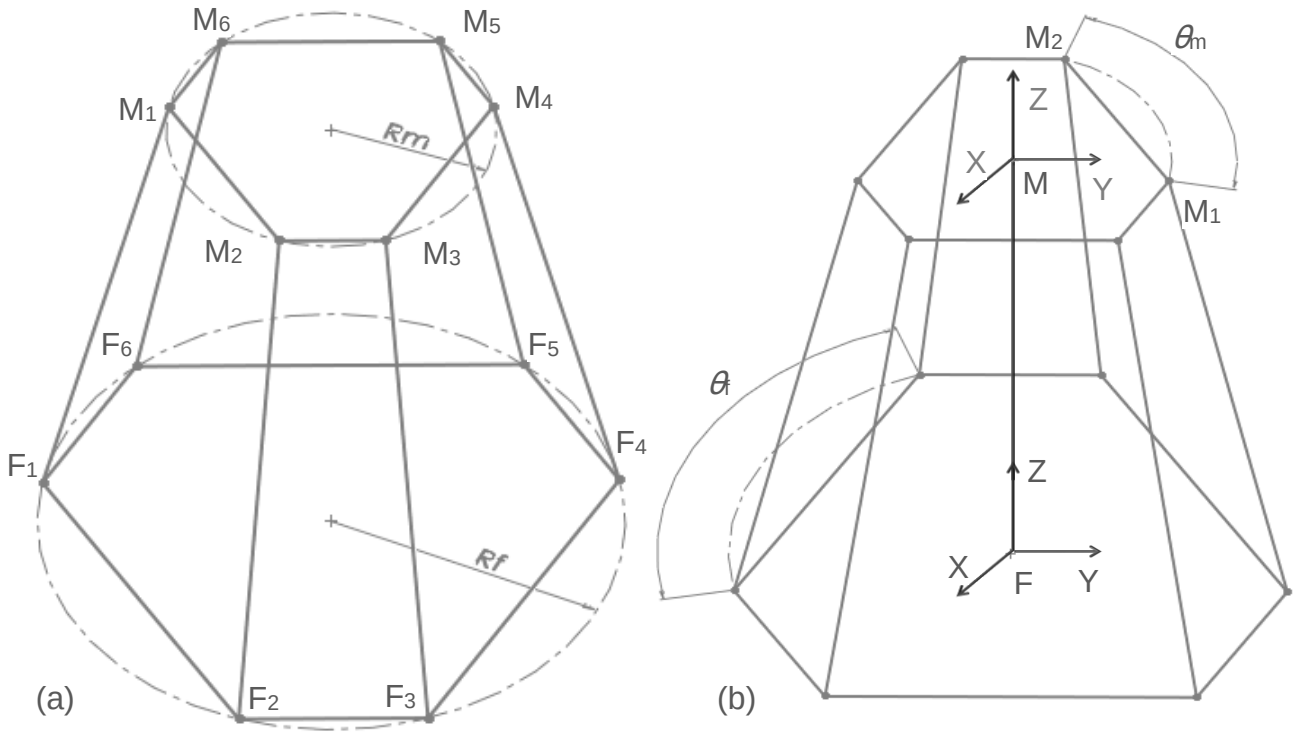

Figure 3.7: The general scheme of the SP and the distribution of the points of contact on the upper and lower platforms

From figure (3.7a) the location of the i^{th} attachment point (M_i) on the moving platform can be found using Equation (3.1).

R_m and R_f are the radius of the moving platform and fixed base, respectively. And by using the same approach, the location of the i^{th} attachment point (F_i) on the base platform can be obtained from the Equation (3.2).

$$GM_i = \begin{bmatrix} GM_{xi} \\ GM_{yi} \\ GM_{zi} \end{bmatrix} = \begin{bmatrix} R_m \cos(\varphi_i) \\ R_m \sin(\varphi_i) \\ 0 \end{bmatrix}, \quad \varphi_i = \frac{i\pi}{3} - \frac{\theta_m}{2} \quad i = 1,3,5 \quad , \quad \varphi_i = \varphi_{i-1} + \theta_m \quad i = 2,4,6 \tag{3.1}$$

$$GF_i = \begin{bmatrix} GF_{xi} \\ GF_{yi} \\ GF_{zi} \end{bmatrix} = \begin{bmatrix} R_f \cos(\tau_i) \\ R_f \sin(\tau_i) \\ 0 \end{bmatrix}, \quad \tau_i = \frac{i\pi}{3} - \frac{\theta_f}{2} \quad i = 1,3,5 \quad , \quad \tau_i = \tau_{i-1} + \theta_f \quad i = 2,4,6 \tag{3.2}$$

Where: GM_i and GF_i are the position vectors.

The pose of the moving platform can be described by a position vector, P and a rotation matrix, ${}^{F}R_{M}$. The rotation matrix is defined by the roll, pitch and yaw angles, which represent rotation of α about the fixed x-axis, $R_X(\alpha)$, followed by a rotation of β about the fixed y-axis, $R_Y(\beta)$ and a rotation of γ about the fixed z-axis, $R_Z(\gamma)$.

In this way, the rotation matrix of the moving platform with respect to the base platform coordinate system is obtained. The position vector P denotes the translation vector of the origin of the moving platform with respect to the base platform. Thus, the rotation matrix and the position vector are given as the following.

$${}^{F}R_{M} = R_Z(\gamma)R_Y(\beta)R_X(\alpha) = \begin{bmatrix} r_{11} & r_{12} & r_{13} \\ r_{21} & r_{22} & r_{23} \\ r_{31} & r_{32} & r_{33} \end{bmatrix} \tag{3.3a}$$

$${}^{F}R_{M} = \begin{bmatrix} \cos\beta\cos\gamma & \cos\gamma\sin\alpha\sin\beta - \cos\alpha\sin\gamma & \sin\alpha\sin\gamma + \cos\alpha\cos\gamma\sin\beta \\ \cos\beta\sin\gamma & \cos\alpha\cos\gamma + \sin\alpha\sin\beta\sin\gamma & \cos\alpha\sin\beta\sin\gamma - \cos\gamma\sin\alpha \\ -\sin\beta & \cos\beta\sin\alpha & \cos\alpha\cos\beta \end{bmatrix} \tag{3.3b}$$

$$P = \begin{bmatrix} P_x & P_y & P_z \end{bmatrix}^T \tag{3.4}$$

In Figure (3.7), the above vectors GM_i and GF_i are chosen as the position vector.

The vector L_i of the link *i* is simply obtained as;

$$L_i = R_{XYZ} GM_i + P - GF_i \qquad i = 1, 2, \ldots, 6 \tag{3.5}$$

When the position and orientation of the moving platform are given $G_{p-o} = \begin{bmatrix} P_x & P_y & P_z & \alpha & \beta & \gamma \end{bmatrix}^T$, the length of each leg is computed by the following equation;

$$\begin{aligned} l_i^2 &= (P_x - GF_{xi} + GM_{xi} r_{11} + GM_{yi} r_{12})^2 \\ &+ (P_y - GF_{yi} + GM_{xi} r_{21} + GM_{yi} r_{22})^2 \\ &+ (P_z - GM_{xi} r_{31} + GM_{yi} r_{32})^2 \end{aligned} \tag{3.6}$$

Where l_i is the scalar value of the length $l_i = \|L_i\|$ which represent the length of the actuators.

3.1.3 Constructing the Stewart Platform Model

By gathering all the parts explained in the Sec. 3.1.1, the SP model was constructed as shown in the Fig (3.8).

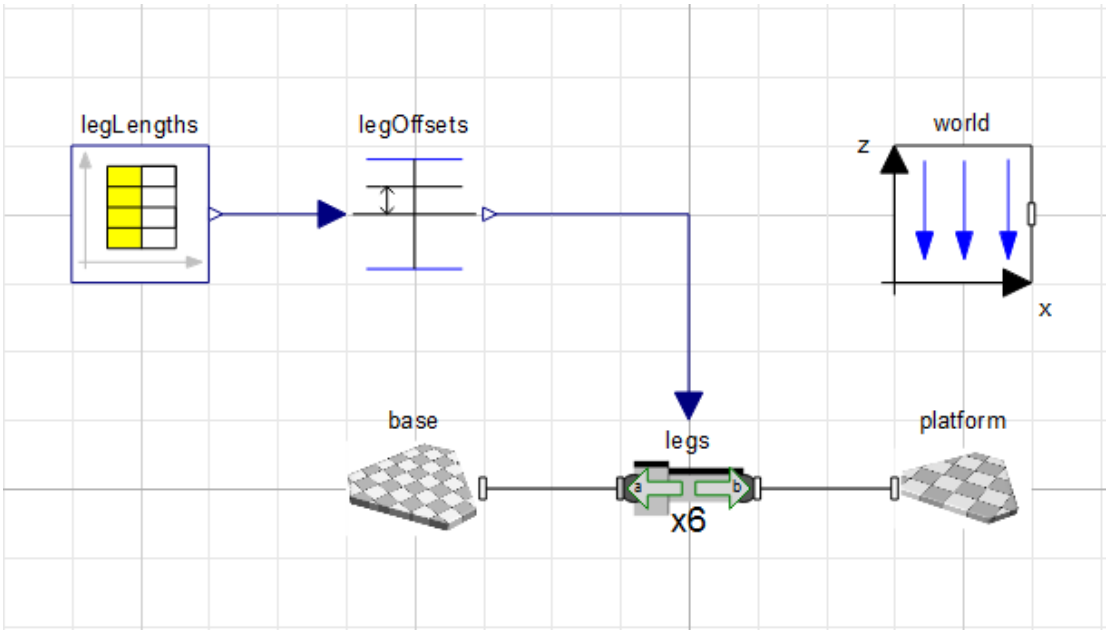

Figure 3.8 : The complete representation of SP parts in System Modeler

After entering the basic data (shape measurement) for each part and connecting them in System Modeler, the whole shape must be connected to Mathematica, where the coding and mathematical equations can be developed to calculate the kinematic motion of the SP movement to allow to represent the movement of each actuator and saving their lengths in a data base.

Through sending the length data to the controller of the prismatic joint of the model, the SP can track the coordinates of the movement to shape the movement of the platform which can be simulated in the simulation center of the Modeler, where more analyzing data can be gotten leading to study the kinematic data of each movement of the platform and compare the different results.

Starting by defining the environment of the model in which it is simulate using the block (world) and defining the value of gravity which is 9.81(m/s^2) in the direction of downward (-z).

After that, the coordinate points of contact between the base and the legs must be calculated using Mathematica and then inserting them into the parameter (leg base point) of the block (base) in Modeler.

$$\left\{\begin{matrix}\{14.48, 3.88, 0\}, \{-3.88, 14.48, 0\}, \{-10.6, 10.6, 0\}, \\ \{-10.6, -10.6, 0\}, \{-3.88, -14.48, 0\}, \{14.48, -3.88, 0\}\end{matrix}\right\}$$

And same thing for the upper platform but the coordinates insert in the (leg platform relative positions) parameter of the (platform) block in Modeler

$$\left\{\begin{matrix}\{7, 7, 17\}, \{2.5, 9.6, 17\}, \{-9.6, 2.5, 17\}, \{-9.6, -2.5, 17\}, \\ \{2.5, -9.6, 17\}, \{7, -7, 17\}\end{matrix}\right\}$$

And then entering the initial height for the platform which is 17 cm. to the modeler,
After that, creating a function in Mathematica to find the pose of the platform that represent the 6DOF $(x, y, z, \theta, \phi, \tau)$ using the translation vector method and rotation matrix with respect to the base. And by using this function the required movement of the platform can be achieved by changing any variable of the six directions to gain the required shape of movement.

Then calculating the length of each leg by using the method in the Sec 3.1.2 and saving these values in a certain file and fed them in to Modeler using the block (leg Lengths)

Fig(3.8), which is connected to the prismatic joint, represent the legs movement according to these lengths to get the shape of the movement required.

And finally through going to the simulation center, the whole model can be simulated in 3D to represent the movement of SP and to be able to get further analysis about the simulation of each leg during the SP movement.

Chapter 4

RESULTS AND DISCUSSION

4.1 Kinematics of the Stewart Platform Model

The Stewart Platform (SP) was aimed to be modelled for predicting knee (tibiofemoral) joint kinematics and the length changes of the knee joint ligaments. The total kinematic mobility of the knee joint was represented by six degrees of freedom (6DOF) as written in Sec. 1.2. The same kinematic mobility was adapted for the top platform of the SP. Therefore the kinematic movement of the SP can mimic the knee joint movement and comprehensive data can be obtained for complete kinematics of the knee joint which is modelled by the SP. The aim here is taking into account the various knee joint movements through considering the tibia as moving body based on its COM. The modelling and simulation of the knee joint with SP was based on the SystemModeler simulation software [17], considering the center of the top platform is the COM for the tibia. Based on this modelling arrangements, the legs of the SP platform represent the main collateral ligaments of the knee joint that leads to determine the changes in the length of the ligaments associated by particular platform movements. A Cartesian coordinate system was used to establish local and global coordinate systems (translations along x, y, and z axes; rotations around axes: α [x axis], β [y axis], and γ [z axis]).

4.1.1 Flexion Movement of the Knee Joint

The knee joint kinematic information has been aimed to be collected based on its flexion-extension movements occur around the angle of β. Firstly, the joint started its flexion movement from 0° and continued up to -30°. The kinematics of the knee joint were obtained based on its flexion angles and time of the movement. According to the flexion movement of the knee joint, the recorded kinematics of the SP model is given in Table 4.1.

In Table 4.1, the length changes of the SP legs were recorded which represent the collateral ligaments of the knee joint.

Table 4.1: The Length Change of the Steward Platform Legs during Knee Joint Flexion

Time (Sec.)	angle(°)	leg 1 (mm)	leg 2 (mm)	leg 3 (mm)	leg 4 (mm)	leg 5 (mm)	leg 6 (mm)
1	0	170	170	170	170	170	170
1.1	3	173.659	171.53	165.923	165.92	171.53	173.65
1.2	6	177.056	172.684	161.56	161.56	172.68	177.05
1.3	9	180.52	173.8	157.28	157.28	173.807	180.52
1.4	12	184.05	174.89	153.1	153.108	174.89	184.08
1.5	15	187.63	175.95	149.05	149.05	175.95	187.63
1.6	18	191.25	176.97	145.14	145.14	176.97	191.25
1.7	21	194.89	177.95	141.405	141.4	177.95	194.89
1.8	24	198.54	178.89	137.85	137.85	178.89	198.54
1.9	27	202.19	179.79	134.52	134.52	179.79	202.19
2	30	205.84	180.64	131.436	131.436	180.64	205.84

The length changes of the SP legs based on the flexion angle β were plotted and shown in Figure 4.1

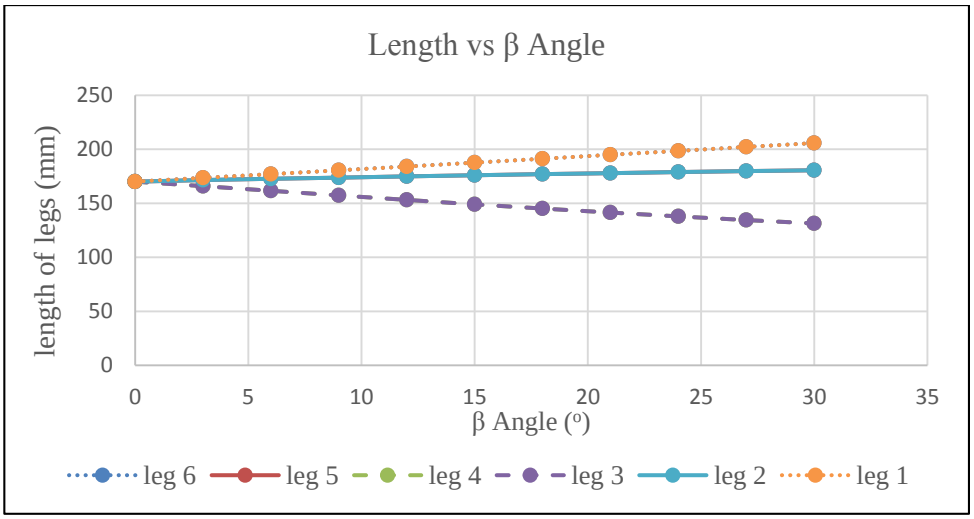

Figure 4.1: The Length Changes of the SP legs vs the flexion angle, β

The SP which represents the knee joint moved in flexion from 0° to -30°. The duration of the total flexion of the knee joint from 0° to -30° took 2 seconds. Therefore, the changes of the leg lengths were also plotted based on time and shown in Fig. 4.2.

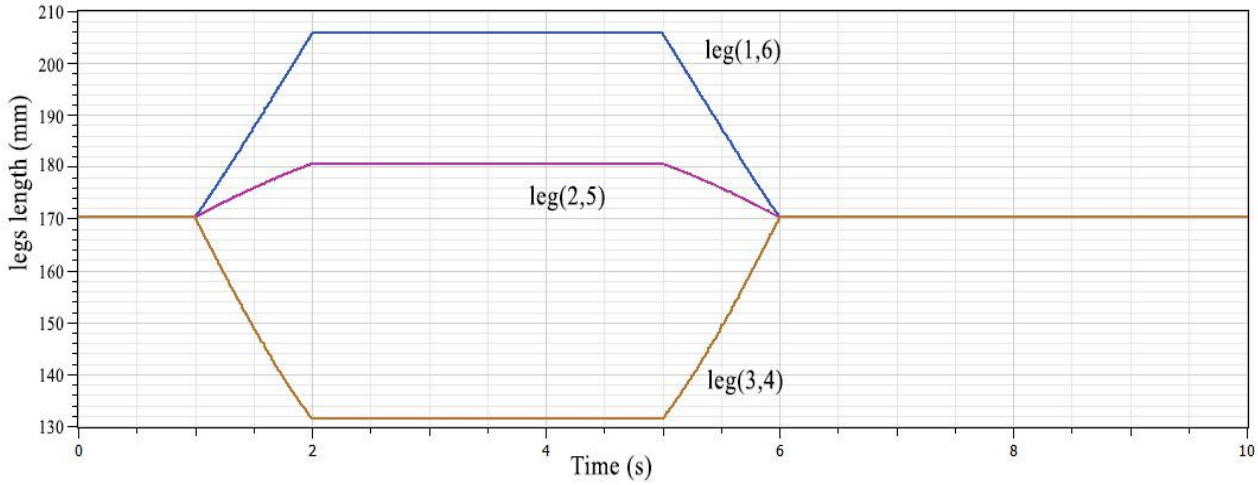

Figure 4.2: The Length Changes of the SP legs vs Time During Knee Joint Model Flexion

Our findings about the ligaments length changes corroborated previous findings in which the leg 3 and leg 4 decreased from 0° to 30° represented the length changes of single bundle ACL [18], some studies have also provided information about the length changes of the PCL [19] [20]. In these studies, it was found that the length of the PCL increased with increasing knee-joint flexion angles. The legs 6 and 5 of the SP showed

the similar increase with the platform leg length changes validated the model of the SP. Previously published studies also highlighted the length changes of the MCL and LCL [21] [22].

Theses MCL and LCL length changes were compared with the SP leg length changes. The decrease of the lengths of the SP legs no. 3 and 4 also validated the representation of the ligaments. As the knee joint model posseses 6DOF, in addition to the flexion-extension rotational movement the varus-valgus and internal-external rotation movements were also recorded. During these rotational movements, the changes in the lengths of the SP legs were also recorded and given in Table 4.2. During the flexion movement of the knee joint from 0° to -30°, it was recorded that the knee moved in valgus rotation from 0° to -2.64°. Again the knee joint kinematics were recorded as the length changes of the SP legs when it moves from 0° to -30° in flexion and from 0° to -2.64° in valgus rotation (Table 4.2). As the knee joint flexion increases the valgus rotation increases as well.

After completing the -30° flexion, the joint was programmed to move in valgus rotation from 0° to -2.64°. As given in Table 4.1, the total duration of the flexion was 2 seconds

and in addition to that, the total duration of the valgus rotation to -2.64° was recorded in 1 seconds (Table 4.2).

Table 4.2: The Length Change of the Steward Platform Legs during Knee Joint Flexion and Valgus Rotation in 4 seconds

Time (sec.)	leg 1 (mm)	leg 2 (mm)	leg 3 (mm)	leg 4 (mm)	leg 5 (mm)	leg 6 (mm)
1	170	170	170	170	170	170
1.1	173.65	171.53	165.92	165.923	171.53	173.659
1.2	177.05	172.68	161.56	161.56	172.684	177.056
1.3	180.52	173.807	157.28	157.28	173.8	180.52
1.4	184.08	174.89	153.108	153.1	174.89	184.05
1.5	187.63	175.95	149.05	149.05	175.95	187.63
1.6	191.25	176.97	145.14	145.14	176.97	191.25
1.7	194.89	177.95	141.4	141.405	177.95	194.89
1.8	198.54	178.89	137.85	137.85	178.89	198.54
1.9	202.19	179.79	134.52	134.52	179.79	202.19
2	205.84	180.64	131.436	131.436	180.64	205.84
3	205.84	180.64	131.436	131.436	180.64	205.84
3.1	205.7	180.4	131.4	131.44	180.8	206
3.2	205.5	180.3	131.4	131.45	181	206.1
3.3	205.36	180	131.4	131.46	181.2	206.3
3.4	205.2	179.9	131.4	131.47	181.38	206.4
3.5	205	179.7	131.4	131.48	181.56	206.6
3.6	204.9	179.5	131.4	131.49	181.74	206.7
3.7	204.7	179.4	131.4	131.5	181.93	206.9
3.8	204.5	179.17	131.4	131.51	182.1	207
3.9	204.4	178.99	131.4	131.53	182.3	207.2
4	204.2	178.8	131.4	131.55	182.5	207.4

The data recorded in Table 4.2 was then plotted and the length changes of the SP legs based on the valgus rotations (α) were plotted and shown in Figure 4.3.

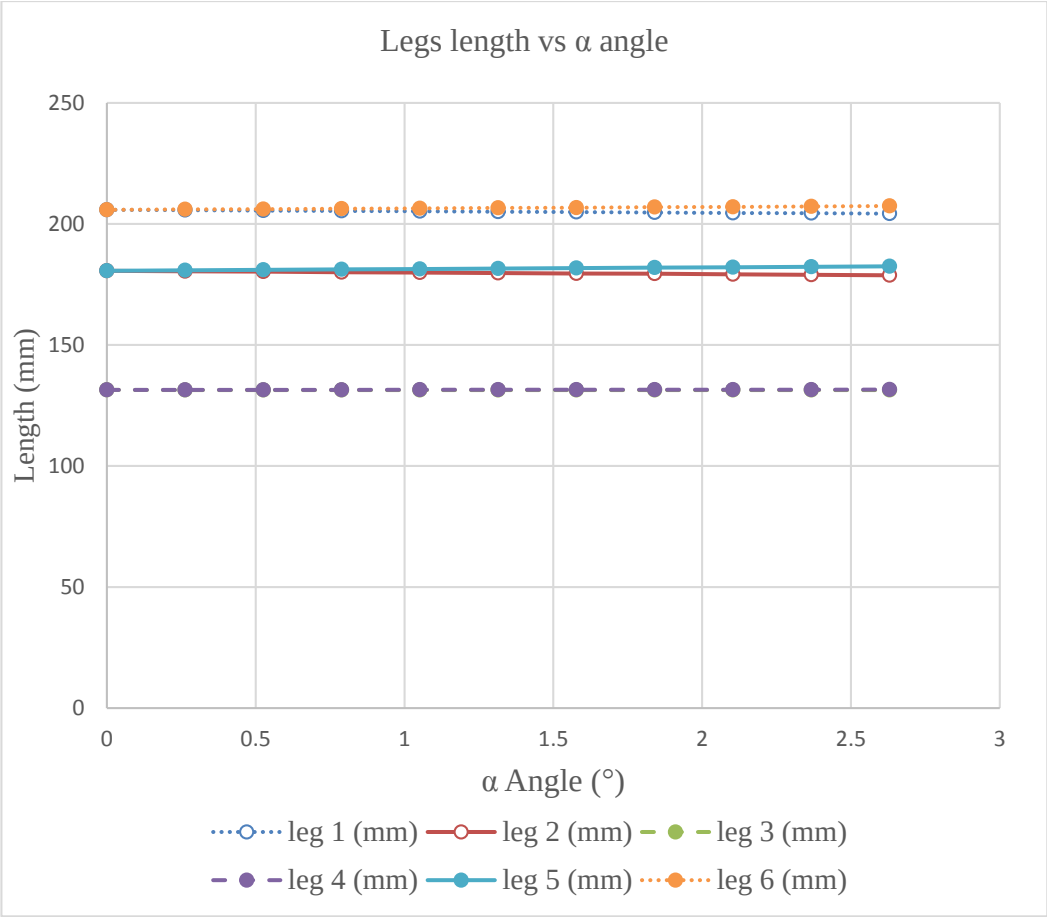

Figure 4.3: The Length Changes of the SP legs During Knee Joint Model Valgus Rotation (α)

The length changes of the SP legs were also plotted during the time of flexion and valgus rotations and shown in Figure 4.4.

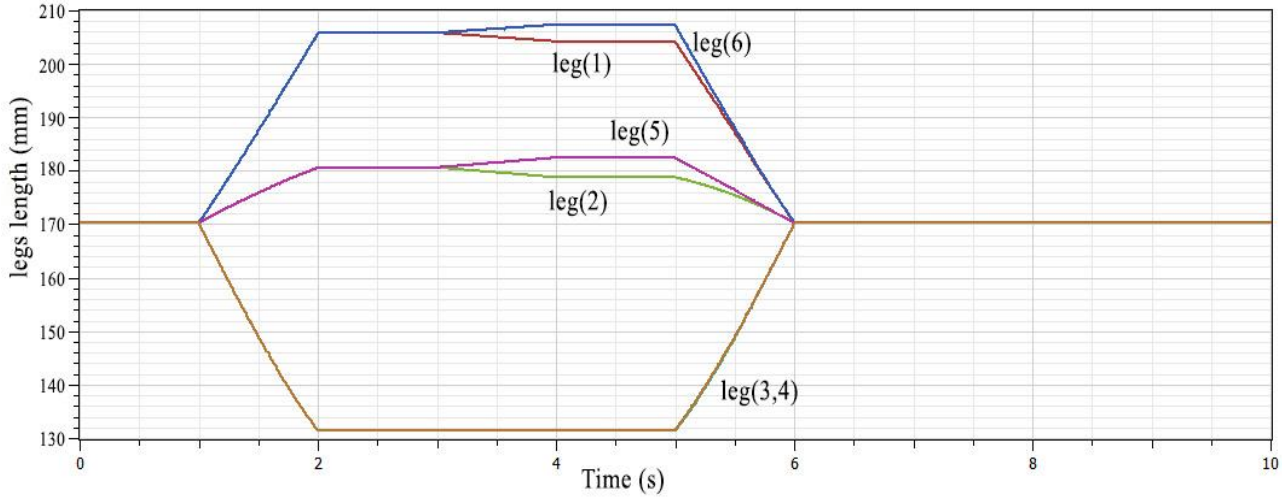

Figure 4.4: The Length Changes of the SP Legs vs Time of flexion and valgus rotations

According to the literature review, it was proved by the researchers that the knee joint performs varus-valgus and internal-external rotations during its flexion.

From the findings of the VV kinematics, it is seen that the results of the SP model showed increase in valgus rotation from 0 to 30. These results were compared with the previously published data [23] and the model's VV rotations were validated. Therefore, in addition to the previously shown Figures from Fig.4.1 to 4.4, the length changes of the SP legs were also plotted according to the internal-external rotations. Based on the literature data, the knee joint model was rotated internally from 0° to 4.2°.

The same procedure was followed to obtain the changes in the lengths of the SP legs during the internal rotation. As seen in Table 4.3, the length changes of the SP legs were recorded from 0 to 2 seconds for flexion rotation, from 2 to 4 seconds for valgus rotation and from 4 to 6 seconds for internal rotation.

Table 4.3: The Length Changes of the SP legs during flexion (β), valgus (α) and internal rotation (γ)

Time (sec.)	leg 1 (mm)	leg 2 (mm)	leg 3 (mm)	leg 4 (mm)	leg 5 (mm)	leg 6 (mm)
1	170	170	170	170	170	170
1.1	173.65	171.53	165.92	165.923	171.53	173.659
1.2	177.05	172.68	161.56	161.56	172.684	177.056
1.3	180.52	173.807	157.28	157.28	173.8	180.52
1.4	184.08	174.89	153.108	153.1	174.89	184.05
1.5	187.63	175.95	149.05	149.05	175.95	187.63
1.6	191.25	176.97	145.14	145.14	176.97	191.25
1.7	194.89	177.95	141.4	141.405	177.95	194.89
1.8	198.54	178.89	137.85	137.85	178.89	198.54
1.9	202.19	179.79	134.52	134.52	179.79	202.19
2	205.84	180.64	131.436	131.436	180.64	205.84
3	205.84	180.64	131.436	131.436	180.64	205.84
3.1	205.7	180.4	131.4	131.44	180.8	206
3.2	205.5	180.3	131.4	131.45	181	206.1
3.3	205.36	180	131.4	131.46	181.2	206.3
3.4	205.2	179.9	131.4	131.47	181.38	206.4
3.5	205	179.7	131.4	131.48	181.56	206.6
3.6	204.9	179.5	131.4	131.49	181.74	206.7
3.7	204.7	179.4	131.4	131.5	181.93	206.9
3.8	204.5	179.17	131.4	131.51	182.1	207
3.9	204.4	178.99	131.4	131.53	182.3	207.2
4	204.2	178.8	131.4	131.55	182.5	207.4
5	204.2	178.8	131.4	131.55	182.5	207.4
5.1	204.2	179.39	131.1	131.86	181.9	207.41
5.2	204.19	179.97	130.7	132.19	181.35	207.45
5.3	204.18	180.56	130.4	132.5	180.7	207.49
5.4	204.16	181.15	130	132.8	180.2	207.5
5.5	204.15	181.74	129.76	133.21	179.6	207.58
5.6	204.14	182.3	129.45	133.55	179.1	207.6
5.7	204.13	182.9	129.15	133.9	178.5	207.68
5.8	204.13	183.52	128.86	134.28	177.96	207.74
5.9	204.12	184.12	128.57	134.65	177.4	207.78
6	204.12	184.7	128.29	135.03	176.84	207.84

The data which is given in Table 4.3 was also plotted in Fig. 4.5. The Fig. 4.5 shows the length changes of the SP legs vs internal rotation (γ).

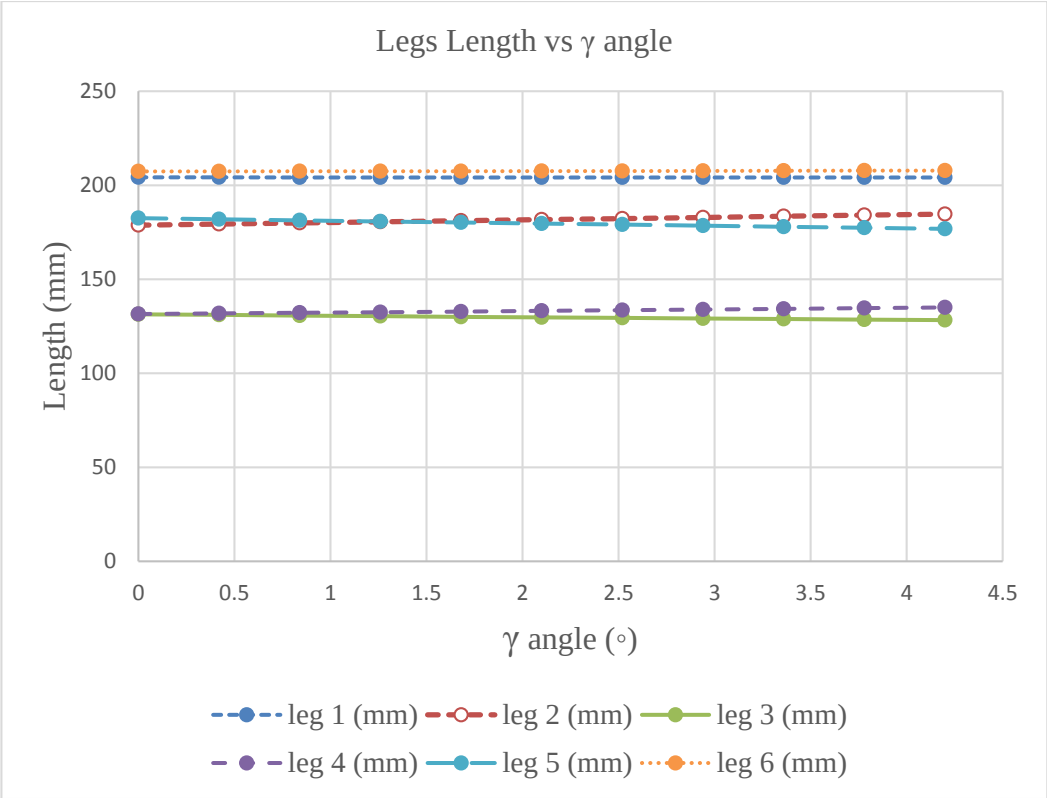

Figure 4.5: The Length Changes of the SP legs During Knee Joint Model Internal Rotation (γ)

The length changes of the SP legs were also plotted during the time of flexion, valgus rotations and internal rotation shown in Figure 4.6.

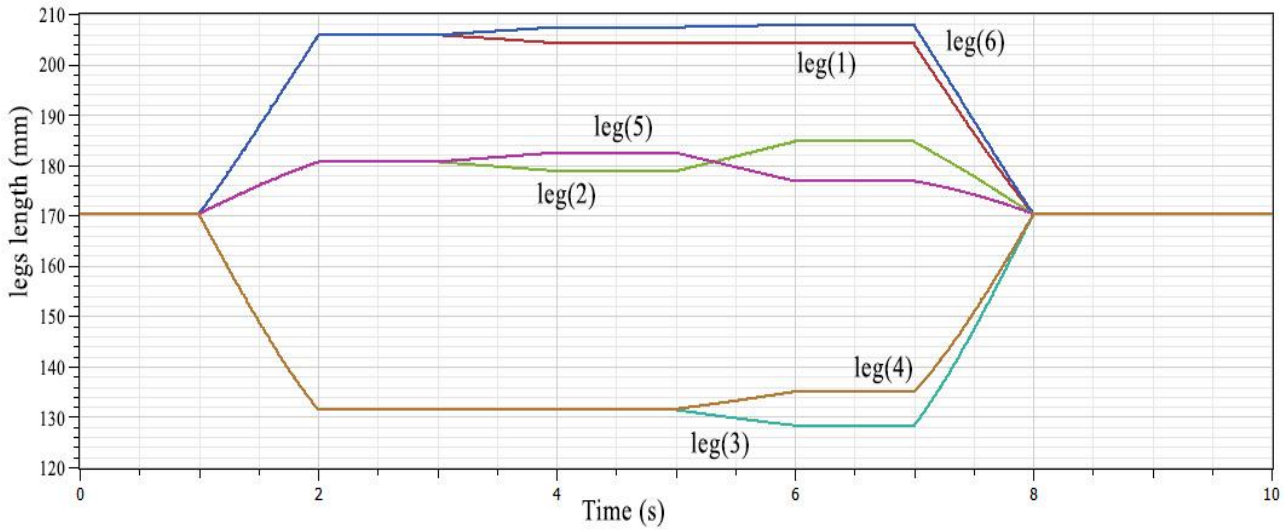

Figure 4.6: The Length Changes of the SP Legs vs Time of flexion and valgus rotations

The Internal-External (IE) rotation kinematics data was also found and imported into the SP model construction. The IE kinematics of the SP model was similar with the published data [24], which showed the validity of the model in IE rotations.

With severe joint and soft tissue injuries, understanding the complete biomechanics of the knee joint and its interactions with surrounding soft tissues is beneficial to improve joint and tissue reconstruction surgery. In this study, the complete kinematics of the knee joint were studied by Steward Platform model which provided significant new contributions to understanding the roles of the SP legs and the ligament lengths implicitly.

Chapter 5

CONCLUSION

Understanding the kinematics of the knee joint and the role of the surrounding ligaments is very important in diagnosis the knee joint behavior during daily life activity and comparing these ligaments length with the length of SP legs length is giving a further knowledge in the knee joint analysis during movement. Therefore, the model of the Steward Platform was used to perform the knee joint kinematic motion within a certain range of movement (0° to 30°) to investigate the similarity between the changes in the platform leg lengths and the knee joint ligament lengths. The initial lengths of the platform legs were adjusted as 17cm at 0° joint flexion and extending up to about 21cm at 30° taking in consideration the COM of the SP as the COM of tibia. It was found that the lengths of the platform legs varied with tibiofemoral flexion angle during 6DOF platform motion. Also it was seen that between 0° to 30° flexion angle, the platform performed valgus rotation dominantly and the leg length of the platform decreased which represented the Anterior Cruciate Ligament (ACL), Medial Collateral Ligament (MCL) and Lateral Collateral Ligament (LCL) length changes.

The average changes of the platform legs were found as 0.119% for platform leg 1, 0.035% for platform leg 2, 0.1285% for leg3, 0.1285% for leg4, 0.035% for leg5 and 0.119% for leg6, from the constructed data of the results, the Steward Platform could mimic the anatomic knee joint kinematics and the platform legs predicted the anatomic knee joint ligament length changes. The kinematics of the platform were validated with

the previously published works [22] [23] [24]. It showed increase in valgus rotation and internal rotations. Therefore, the SP leg changes were found easier to be compared with the previously published data on knee ligament length changes [18-22].

Our findings showed that the SP can mimic the kinematics of the knee joint and the ligament length changes.

In this modelling study, the kinematics of the knee joint was restricted to save time in simulation. However the results that were obtained were validated by the published works which show the future work possibilities in developing the SP model includes higher degrees of knee translations and rotations. This kind of studies are helpful to develop orthopaedic implants as well as the orthopaedic surgeries. Through simulating accurate knee joint kinematics and ligament length changes will also improve the technologies in orthopaedics.

REFERENCES

[1] P. Gomes, "Surgical robotics: Reviewing the past, analysing the present, imagining the future," *Robotics and Computer-Integrated Manufacturing*, vol. 27, p. 261–266, 2011.

[2] F. Pugin, P. Bucher, P. Morel, "History of robotic surgery : From AESOP® and ZEUS® to da Vinci®," *Journal of Visceral Surgery*, vol. 148, p. e3—e8, 4 October 2011.

[3] M. F. Dror Paley, "History and Science Behind the Six-Axis Correction External Fixation Devices in Orthopaedic Surgery," *Operative Techniques in Orthopaedics*, vol. 21, pp. 125-128, 2011.

[4] "Geomagic website," Geomagic, [Online]. Available: http://www.geomagic.com. [Accessed 27 October 2014].

[5] Scott L. Delp, Frank C. Anderson, Allison S. Arnold, Peter Loan, Ayman Habib, Chand T. John, Eran Guendelman, and Darryl G. Thelen, "OpenSim: Open-Source Software to Create and Analyze Dynamic Simulations of Movement," *IEEE Transactions on Biomedical Engineering*, Vols. 54, NO. 11, pp. 1940-1950, NOVEMBER 2007.

[6] "Opensim program," [Online]. Available: http://opensim.stanford.edu. [Accessed 27 October 2014].

[7] D. Zhang, Parallel Robotic Machine Tools, Faculty of Engineering and Applied Science University of Ontario Institute of Technology (UOIT) Oshawa, ON Canada: Springer Science+Business Media, 2010.

[8] Gough VE, Whitehall SG, "Universal tire test machine," *Proceedings of the FISITA Ninth International Technical Congress*, pp. 117-137, May, 1962.

[9] I. Bonev, "The True Origins of Parallel Robots," 24 January January 24, 2003. [Online]. Available: http://www.parallemic.org/Reviews/Review007.html.

[10] J.-P. MERLET, Parallel Robots (Second Edition), INRIA, Sophia-Antipolis, France: Springer, 2006.

[11] D.Stewart, "A platform with six degrees of freedom," *Proceedings of the IMechE,* Vols. 180, Pt. 1, No. 15, pp. 371-385, 1965.

[12] "SIMM website," MusculoGraphics, Inc, [Online]. Available: http://www.musculographics.com/html/products/SIMM.html. [Accessed 27 October 2014].

[13] "SliceOmatic website," TomoVision, 3280 chemin Milletta, Magog, J1X 0R4, Canada, [Online]. Available:

http://www.tomovision.com/products/sliceomatic.html. [Accessed 27 October 2014].

[14] C. Canudas de Wit, B. Siciliano, G. Bastin, Theory of Robot Control, London : Springer, 1996.

[15] J.G. Ziegler, N.B. Nichols, "Optimum settings for automatic controllers," *ASME Trans.*, vol. 64, p. 759–768, 1942.

[16] Y. Choi, W.K. Chung, "PID Trajectory Tracking Control for Mechanical Systems," *Lecture Notes in Control and Information Sciences*, vol. 289, 2004.

[17] "Wolfram company website," Wolfram, [Online]. Available: http://www.wolfram.com. [Accessed 27 October 2014].

[18] Yoo, Y.S., Jeong, W.S., Shetty, N.S., Ingham, S.J.M., Smolinski, P., Fu, F., "Changes in ACL length at different knee flexion angles: an in vivo biomechanical study," *Knee Surg. Sports Traumatol Arthrosc.*, vol. 18, no. 3, pp. 292-297, 2010.

[19] Bowman, K.F., Sekiya, J.K., "Anatomy and biomechanics of the posterior cruciate ligament and other ligaments of the knee," *Oper Tech Sports Med.*, vol. 17, no. 3, pp. 126-134, 2009.

[20] Ahmad, C.S., Cohen, Z.A., Levine, W,N., Gardner, T.R., Ateshian, G.A., Mow, V.C., "Codominance of the individual posterior cruciate ligament bundles," *Am J Sports Med.*, vol. 31, no. 2, pp. 221-225, 2003.

[21] Bergamini, E., Pillet, H., Thoreux, P., Guerard, S., Camomilla, V., Cappozzo, A., Skalli, W., "Tibio-femoral joint constraints for bone pose estimation during movement using multi-body optimization," *Gait & Posture,* vol. 33, no. 4, pp. 706-711, 2011.

[22] Sang Eun Park, Louis E. DeFrate, Jeremy F. Suggs, Thomas J. Gill, Harry E. Rubash, Guoan Li, "Erratum to The change in length of the medial and lateral collateral ligaments during in vivo knee flexion," *The Knee* , vol. 13, no. 1, p. 77 – 82, 2006.

[23] Van den Bogaerde, J.M., Shin, E., Neu, C.P., and Marder, R.A., "The superficial medial lateral ligament reconstruction of the knee: effect of altering graph length on knee kinematics and stability," *Knee Surg. Traumatol. Arthrosc.*, vol. 19, no. 1, pp. S60-S66, 2011.

[24] E. Most, J. Axe, H. Rubash, G. Li, "Sensitivity of the knee joint kinematics calculation to selection of flexion axes," *Journal of Biomechanics,* vol. 37, no. 11, p. 1743–1748, 2004.

[25] S. Küçük, Serial and Parallel Robot Manipulators – Kinematics, Dynamics, Control and Optimization, Janeza Trdine 9, 51000 Rijeka, Croatia: InTech, 2012.

[26] S. W. Yamin Wan, "Kinematics Analysis and Simulation System Realization of Stewart Platform Manipulator," in *The Fourth International Conference on Control and Automation (ICCA'03)*, Montreal, Canada, 10-12 June 2003.

[27] Marcial Trilha Junior, Eduardo Alberto Fancello, Carlos Rodrigo de Mello Roesler and Ari Digiácomo Ocampo More, "Three Dimensional Numerical Simulation of Human Knee Joint Mechanics," *Acta Ortop Bras.,* pp. 18-23, 2009; 17(2).

[28] J. E. Lang, S. Mannava, A. J. Floyd, M. S. Goddard, B. P. Smith, A. Mofidi, T. M. Seyler, R. H. Jinnah, "Robotic systems in orthopaedic surgery," *The Journal of Bone and Joint Surgery,* Vols. 93-B, No. 10, p. 1296–1299, OCTOBER 2011.

[29] Kai Liu, John M. Fitzgerald and Frank L. Lewis, "Kinematic Analysis of a Stewart Platform Manipulator," *IEEE Transactions on Industrial Electronics,* Vols. 40, NO. 2, pp. 282-293, APRIL 1993.

[30] Yangjun Pi n, XuanyinWang, "Trajectory tracking control of a 6-DOF hydraulic parallel robot manipulator with uncertain load disturbances," *Control Engineering Practice,* vol. 19, p. 185–193, 2011.

[31] Bhaskar Dasgupta, T.S. Mruthyunjaya, "The Stewart platform manipulator: a review," *Mechanism and Machine Theory,* vol. 35, pp. 15-40, 2000.

[32] Hiroshi Takemura1, Takayuki Onodera, Ding Ming and Hiroshi Mizoguchi, "Design and Control of a Wearable Stewart Platform-Type Ankle-Foot Assistive Device," *International Journal of Advanced Robotic Systems ,* Vols. 9, 202, 2012.

[33] J. J. Craig, Introduction to Robotics Mechanics and Control, United States of America: Pearson Education, Inc., 2005.

[34] Bruno Siciliano, Oussama Khatib, Handbook of Robotics, United States of America: Springer, 2008.

[35] David B. Camarillo, Thomas M. Krummel, J. Kenneth Salisbury,, "Robotic technology in surgery: past, present, and future," *The American Journal of Surgery,* vol. 188 , p. 2S–15S, October 2004.

[36] Ryszard Jablonski, Mateusz Turkowski, Roman Szewczyk, "The Design of the Device for Cord Implants Tuning," in *Recent Advances inMechatronics*, New York, Springer-Verlag Berlin Heidelberg, 2007, pp. 195-199.

[37] Bozidar Potocnik, Damjan Zazula, Boris Cigale, Dusan Heric, Edvard Cibula and Tomaz Tomazic, "A Patient-specific Knee Joint Computer Model Using MRI Data and ‘in vivo’ Compressive Load fromtheOpticalForce Measuring System,"

Journal of Computing and Information Technology, vol. 16, p. 209–222, 2008, 3.

[38] Yuhua Song, Richard E. Debski, Volker Musahl, Maribeth Thomas, Savio L.-Y. Woo, "A three-dimensional finite element model of the human anterior cruciate ligament:a computational analysis with experimental validation," *Journal of Biomechanics*, vol. 37, p. 383–390, 2004.

[39] P.J. Rowe, C.M. Myles, C. Walker, R. Nutton, "Knee joint kinematics in gait and other functional activities measured using flexible electrogoniometry: how much knee motion is sufficient for normal daily life?," *Gait and Posture* , vol. 12 , p. 143–155, 2000.

[40] Miyasaka KC, Daniel DM, Stone ML, Hirshman P., "The incidence of knee ligament injuries in the general population," *Am J Knee Surg*, vol. 4, pp. 3-8, 1991.

[41] E. Pena , B. Calvo, M.A. Martınez, M. Doblare, "A three-dimensional finite element analysis of the combined behavior of ligaments and menisci in the healthy human knee joint," *Journal of Biomechanics*, vol. 39, p. 1686–1701, 2006.

[42] William D McLeod and Stewart Hunter, "Biomechanical Analysis of the Knee: Primary Functions as Elucidated by Anatomy," *Phys Ther.*, vol. 60, pp. 1561-1564, 1980.

[43] Savio L-Y. Woo, Richard E. Debski, John D. Withrow, and Marsie A. Janaushek, "Biomechanics of Knee Ligaments," *The American Journal of Sports Medicine*, vol. 27, no. 4, pp. 533-543, 1999.

[44] Jeffrey A. Weiss and John C. Gardiner, "Computational Modeling of Ligament Mechanics," *Critical Reviews™ in Biomedical Engineering,* vol. 29, no. 4, p. 1–70, 2001.

[45] Kok-Meng Lee n, Jiajie Guo, "Kinematic and dynamic analysis of ananatomically based knee joint," *Journal of Biomechanics*, vol. 43, p. 1231–1236, 2010.

APPENDIX

Appendix: Thesis code

```
baseTriangleAngles = {0,120,240};
baseTruncationAngle = 15;
baseAngles = SortBy[Flatten[ Table[Mod[{θ + baseTruncationAngle, θ
                    − baseTruncationAngle},360]°, {θ, baseTriangleAngles }],1], Less]
baseRadius = 15;
      basePoints = Table[{ baseRadiusCos[θ],0, baseRadiusSin[θ]}, { θ, baseAngles}]
WSMSetValues[" StewartPlatform. Components. Base", {"legBasePoints" → basePoints}]
platformTriangleAngles = baseTriangleAngles + 60
platformTruncationAngle = 15;
platformAngles
= SortBy[ Flatten[Table[ Mod[{θ + platformTruncationAngle, θ
− platformTruncationAngle},360]°, {θ, platformTriangleAngles}],1], Less]
platformRadius = 10;
relativePlatformPoints
= Table[ {platformRadiusCos[θ],0, platformRadiusSin [θ]}, {θ, platformAngles}]
WSMSetValues ["StewartPlatform. Components. Platform", {"legPlatformRelativePositions"
→ relativePlatformPoints}]
platformHeight = 17;
platformPoints = Table[ p + {0, platformHeight, 0}, {p, relativePlatformPoints}]
platformThickness= 1;
LineSign[{a_,b_}][p_]:=Sign[First [RotationTransform[{b-a,{0,1}}][p-a]]]
      PolygonPredicate [Polygon[pts_],{x_,y_}]:=Apply[And,Table[LineSign[pair][{x,y}]=-
                                                1,{pair,Partition[Append[pts,First[pts]],2,1]}]]
platformPolygon = Polygon[platformPoints 〚All, {1,3}〛 ];
```

platformM

$=$ platformD

$*$ Integrate[Boole[PolygonPredicate[platformPolygon, $\{x, y\}$]&& $\frac{-\text{platformThickness}}{2}$

$< z <$ $\frac{\text{platformThickness}}{2}$], $\{x, -\infty, \infty\}, \{y, -\infty, \infty\}, \{z, -\infty, \infty\}$]

MomentOfInertia[ρ_, {x_, y_, z_}]

$:=$ Integrate[$\rho((x^2 + y^2 + z^2)$IdentityMatrix[3]

$- \{\{x^2, xy, xz\}, \{xy, y^2, yz\}, \{xz, yz, z^2\}\}), \{x, -\infty, \infty\}, \{y, -\infty, \infty\}, \{z, -\infty, \infty\}$]

platformInertia

$=$ MomentOfInertia[platformD

$*$ Boole[PolygonPredicate[platformPolygon, $\{x, y\}$]&& $\frac{-\text{platformThickness}}{2} < z$

$<$ $\frac{\text{platformThickness}}{2}$], $\{x, y, z\}$]//Chop

WSMSetValues["StewartPlatform. Components. Platform", {"mass"

→ platformM, "inertiaTensor" → platformInertia, "platformHeight"

→ platformHeight}]

legLengths $=$ Map[Norm, platformPoints $-$ basePoints]

legDirections $=$ Map[Normalize, platformPoints $-$ basePoints]

WSMSetValues["StewartPlatform. Components. Legs", {"initialLengths"

→ legLengths, "legDirections" → legDirections}]

checkerboard $=$ ConstantArray[Range[$-$baseRadius, baseRadius, $\frac{\text{baseRadius}}{4}$],2];

platformGraphics

$=$ RegionPlot3D[Evaluate[PolygonPredicate[platformPolygon, $\{x, y\}$]&&

$-$ $\frac{\text{platformThickness}}{2} < z$

$<$ $\frac{\text{platformThickness}}{2}$], $\{x, -\text{platformRadius}, \text{platformRadius}\}, \{y, -\text{platformRadius}, \text{platformRadius}\},$

{z, −platformThickness, platformThickness}, BoxRatios → Automatic, PlotPoints

→ 50, Mesh → checkerboard, MeshFunctions → {#3&, #1&}, MeshShading

→ {{GrayLevel[0.6], GrayLevel[0.7]}, {GrayLevel[0.7], GrayLevel[0.6]}}, Lighting

→ "Neutral"]

PoseLegEndpoints[{x_, y_, z_, θ_, ϕ_, τ_}]

:= Table[Composition[TranslationTransform[{x, y, z}

+ {0,0, platformHeight}], RotationTransform[{{0,1,0}, {Sin[θ]Cos[ϕ], Cos[θ], Sin[θ]Sin[ϕ]}}],

RotationTransform[τ, {0,1,0}]][p], {p, relativePlatformPoints}]

PoseLegLengths[pose_]: = Map[Norm, PoseLegEndpoints[N[pose]] − basePoints]

PoseRange[{pose1_, pose2_}, steps_]:

$$= \text{Table}[\text{pose1} + t(\text{pose2} - \text{pose1}), \{t, \text{Range}[0,1, \frac{1}{\text{steps}}]\}]$$

ExportMotionPlan [poses_List,legoffsets_:{0,0,0,0,0,0}] := Module[{framerate

= 10, lengths, tabledata}, lengths = {First[poses]}; Do[lengths

= Join[lengths, Rest@PoseRange[{Last[lengths], wp}, framerate]], {wp, Rest[poses]}];

AppendTo[lengths, Last[lengths]]; lengths = Map[PoseLegLengths, lengths]; lengths

$$= \text{Map}[\# + \text{legoffsets}\&, \text{lengths}]; \text{tabledata}$$

$$= \text{MapIndexed}\left[\text{Prepend}\left[\#, \frac{\text{First}[\#2] - 1}{\text{framerate}}\right]\&, \text{lengths}\right];$$

{Export[FileNameJoin[{NotebookDirectory[ ], "DocumentationFiles", "PlatformPath. txt"}],

{{"LegLengths", tabledata} }, "ModelicaCombiTimeTable"], First[Last[tabledata]]}]

MotionPlan = Block[

{0,0,0,0,0,0},

{0,0,0,0,0,0},

{0,0,0,0, −30°, 0}

{0,0,0,0, −30°, 0}

{0,0,0,0, −30°, 0}

{0,0,0,0, −30°, 0}

$\{0,0,0,-2.63°,-30°,0\}$

$\{0,0,0,-2.63°,-30°,0\}$

$\{0,0,0,-2.63°,-30°,0\}$

$\{0,0,0,-2.63°,-30°,0\}$

$\{0,0,0,-2.63°,-30°,4.2°\}$

$\{0,0,0,-2.63°,-30°,4.2°\}$

$\{0,0,0,-2.63°,-30°,4.2°\}$

$\{0,0,0,-2.63°,-30°,4.2°\}$

{0,0,0,0,0,0},

{0,0,0,0,0,0}}];

$ExportMotionPlan[thirdMotionPlan];$